Available online at www.sciencedirect.com
ScienceDirect
Geochimica et Cosmochimica Acta 71 (2007) 5244–5266
Geochimica et Cosmochimica Acta
www.elsevier.com/locate/gca

Element mobility in mafic and felsic ultrahigh-pressure metamorphic rocks during continental collision

Zi-Fu Zhao *, Yong-Fei Zheng, Ren-Xu Chen, Qiong-Xia Xia, Yuan-Bao Wu

CAS Key Laboratory of Crust–Mantle Materials and Environments, School of Earth and Space Sciences, University of Science and Technology of China, Hefei 230026, China

Received 21 December 2006; accepted in revised form 10 September 2007; available online 25 September 2007

Abstract

In order to decipher element mobility in ultrahigh-pressure (UHP) eclogite-facies metamorphic rocks during subduction and exhumation of continental crust, major-trace elements and Sr–Nd isotopes were systematically investigated for two continuous core segments of about 3 m length from the Chinese Continental Scientific Drilling (CCSD) project in the Sulu orogen. The segments are composed of lithological transitions between UHP eclogite and granitic gneiss. The eclogite exhibits a large variation in major and some trace elements such as LILE (e.g., Rb, Ba and K) and LREE, but a relatively limited range in HFSE and HREE. This suggests high mobility of LILE and LREE but immobility of HFSE and HREE during continental collision-zone metamorphism. Some eclogites have andesitic compositions with high SiO_2, alkalis, LREE, and LILE but low CaO, MgO and FeO contents. These features likely result from chemical exchange with gneisses, possibly due to the metasomatism of felsic melt produced by partial melting of the associated gneisses during the exhumation. On the other hand, some eclogites appear to have geochemical affinity to refractory rocks formed by melt extraction as evidenced by strong LREE and LILE depletion and the absence of hydrous minerals. These results provide evidence of melt-induced element mobility in the UHP metamorphic rocks. In particular, large variations in the abundance of such elements as SiO_2, LREE and LILE occur at the contact between eclogite and granitic gneiss, indicating their mobility between different slab components. Petrographic observations also show the presence of felsic veins on small scales in the UHP metamorphic rocks, demonstrating the occurrence of hydrous melt in local open-systems during the continental collision. As a whole, nevertheless, the protolith nature dictates the geochemical differences in both eclogite and granitic gneiss between the two core segments because mass transport during the subduction-zone metamorphism is principally dictated by the lithological differences at contact. The eclogite and granitic gneiss from the first core segment have high $\varepsilon_{Nd}(t)$ values, whereas those from the second core segment show relatively low $\varepsilon_{Nd}(t)$ values in concordance with majority of UHP metaigneous rocks outcropped along the Dabie–Sulu orogenic belt. Thus contrasting origins of bimodal igneous rocks were involved in the continental collision, demonstrating that the subducted continental crust is the magmatic product of active rifting margin during supercontinental breakup in the middle Neoproterozoic.
© 2007 Elsevier Ltd. All rights reserved.

1. INTRODUCTION

It is often assumed that subducting oceanic crust undergoes extensive dehydration during eclogite-facies metamorphism, with significant removal of water-soluble elements such as large ion lithospheric elements (LILE) and light rare earth elements (LREE) relative to water-insoluble elements such as high field strength elements (HFSE) and heavy rare earth elements (HREE). This paradigm has been used to explain the characteristic enrichment of LILE and LREE but depletion of HFSE in island arc magmas (e.g., Hawkesworth et al., 1991; Tatsumi and Eggins, 1995). A study of element mobility by dehydration experiments during a transition of amphibolite to ultrahigh-pressure (UHP)

* Corresponding author. Fax: +86 551 3603554.
E-mail address: zfzhao@ustc.edu.cn (Z.-F. Zhao).

0016-7037/$ - see front matter © 2007 Elsevier Ltd. All rights reserved.
doi:10.1016/j.gca.2007.09.009

eclogite indeed indicates that LILE and LREE are more readily transported by aqueous fluid during open-system dehydration processes (Kogiso et al., 1997). By comparing the composition of high-pressure (HP) metamorphic rocks to their protoliths, a number of studies indicate considerable removal of LILE and/or LREE from metabasites during subduction up to eclogite-facies conditions (e.g., Arculus et al., 1999; Becker et al., 2000; Scambelluri et al., 2001; John et al., 2004). In contrast, other studies suggest that mafic rocks do not lose significant amounts of trace elements during HP metamorphism up to eclogite-facies (e.g., Chalot-Prat et al., 2003; Spandler et al., 2003, 2004; Volkova et al., 2004). This implies the decoupling between dehydration and loss of trace elements during prograde metamorphism of oceanic crust. Therefore, it has been intriguing how elements are liberated from subducting crusts. This principally concerns the degree and mechanism of element transport with respect to open or closed systems during prograde HP–UHP metamorphism in oceanic subduction zones. Because high solubilities of trace elements may occur in hydrous melt and supercritical fluid, their occurrence or not during subduction-zone metamorphism may have play a critical role in dictating the coupling or decoupling.

Since coesite was identified in metamorphic rocks from the Western Alps (Chopin, 1984), and the Western Gneiss Region of Norway (Smith, 1984), much attention has been paid to UHP metamorphism of continental crust. A series of UHP terranes have been identified in the world, the largest being the Dabie–Sulu orogenic belt among twenty two recognized UHP belts (Ernst and Liou, 1999; Liou, 1999; Carswell and Compagnoni, 2003). The Dabie–Sulu orogenic belt is located at the convergent plate boundary between the North China Block and the South China Block in east-central China (Cong, 1996; Liou et al., 1996; Li et al., 1999; Zheng et al., 2005a), with occurrence of UHP index minerals such as coesite and microdiamond (Okay et al., 1989; Wang et al., 1989; Xu et al., 1992, 2003, 2005). Dabie–Sulu UHP rocks were once supracrustal rocks on the continental crust, that were subducted to mantle depths of >120 km and subsequently rapidly exhumed back to crustal levels (e.g., Liou et al., 1996; Jahn et al., 2003; Zheng et al., 2003). They have recorded various geological processes during deep subduction of the continental crust and subsequent exhumation. Therefore, the Dabie–Sulu orogenic belt is an important locality for studying the geochemical behavior of elements and isotopes during continental subduction-zone metamorphism.

By means of SIMS analysis, Sassi et al. (2000) investigated trace element distribution in minerals from UHP eclogites in the Dabie orogen. Their results indicate that the minerals have consistent trace element compositions and partition coefficients indicative of mutual equilibrium and that no change in the trace element compositions occurs in association with a retrograde recrystallization from the coesite to quartz stability field during exhumation of the deeply subducted continental crust. Mineral O isotope studies of Dabie–Sulu UHP metamorphic rocks have also demonstrated limited mobilities of aqueous fluid across lithological boundaries within UHP slabs (Rumble et al., 2003; Zheng et al., 2003). On the other hand, SIMS zircon U–Pb dating for UHP eclogites and gneisses outcropped along the Dabie–Sulu orogenic belt yields two groups of ages at 242 ± 2 Ma and 227 ± 2 Ma, respectively (Liu et al., 2006; Wu et al., 2006a). They are interpreted to register two episodes of the growth of metamorphic zircons in the prograde HP to UHP stage during the final subduction and the retrograde UHP to HP stage during the initial exhumation, respectively, in response to two episodes of fluid availability during the continental collision (Wu et al., 2006a). Furthermore, Xiao et al. (2006a) observed that rutile from eclogite in the Sulu orogen show highly variable Nb/Ta ratios of 5.4–29.1 within single grains, and interpreted them as fluid-assisted fractionation during continental subduction. A geochemical study of the Dabie–Sulu eclogites by Tang et al. (2007a) demonstrates that LILE had high mobility but REE and HFSE were immobile during the UHP metamorphism.

Although the continental crust is poor of water relative to the oceanic crust, trace amounts of aqueous fluid are still present in the subducting minerals. This provides a potential to decipher element mobility in continental subduction-zone metamorphism. By taking the advantage of having depth profiles between contrasting lithologies from core samples of the Chinese Continental Scientific Drilling (CCSD) project, we have conducted a combined study of petrography, major and trace elements, and Sr and Nd isotopes in UHP eclogite and granitic gneiss from the Sulu orogen. The results provide insight into the relationship between element mobility and melt availability in the processes of continental collision.

2. GEOLOGICAL SETTING AND SAMPLES

The CCSD project provides us with an opportunity to sample UHP cores continuously from great depths up to 5158 m (Xu et al., 1998, 2006). Main and pilot holes of the CCSD are located in Donghai County of Jiangsu Province in the southwestern part of the Sulu orogen (Fig. 1). Metamorphic rocks recovered are various types of gneiss, eclogite, amphibolite, marble and peridotite. Coesite was found as inclusions within zircons from both gneiss and eclogite (Liu et al., 2001, 2002, 2004a,b, 2005; Zhang et al., 2006a), demonstrating that both metagranite and metabasite were subjected to in situ UHP metamorphism. *P–T* estimates of 675–815 °C and 3.1–4.4 GPa were obtained for the eclogites at depths of 0–2050 m from the main hole (MH) of CCSD (Zhang et al., 2006a). Microdiamond was identified in surface-exposed eclogite at Maobei, the CCSD-MH site (Xu et al., 1998, 2003, 2005). SHIRMP U–Pb dating was made for coesite-bearing domains of zircons from gneiss of CCSD cores (Liu et al., 2004a,b, 2005; Liu and Xu, 2004), yielding concordant ages of 234 to 226 Ma for the UHP metamorphic event and about 750–780 Ma for protolith magmatism of the metaigneous rocks. A combined study of petrography and geochronology for the CCSD-MH eclogite also reveals occurrence of HP eclogite-facies recrystallization phase at 216 ± 3 Ma (Zhao et al., 2006).

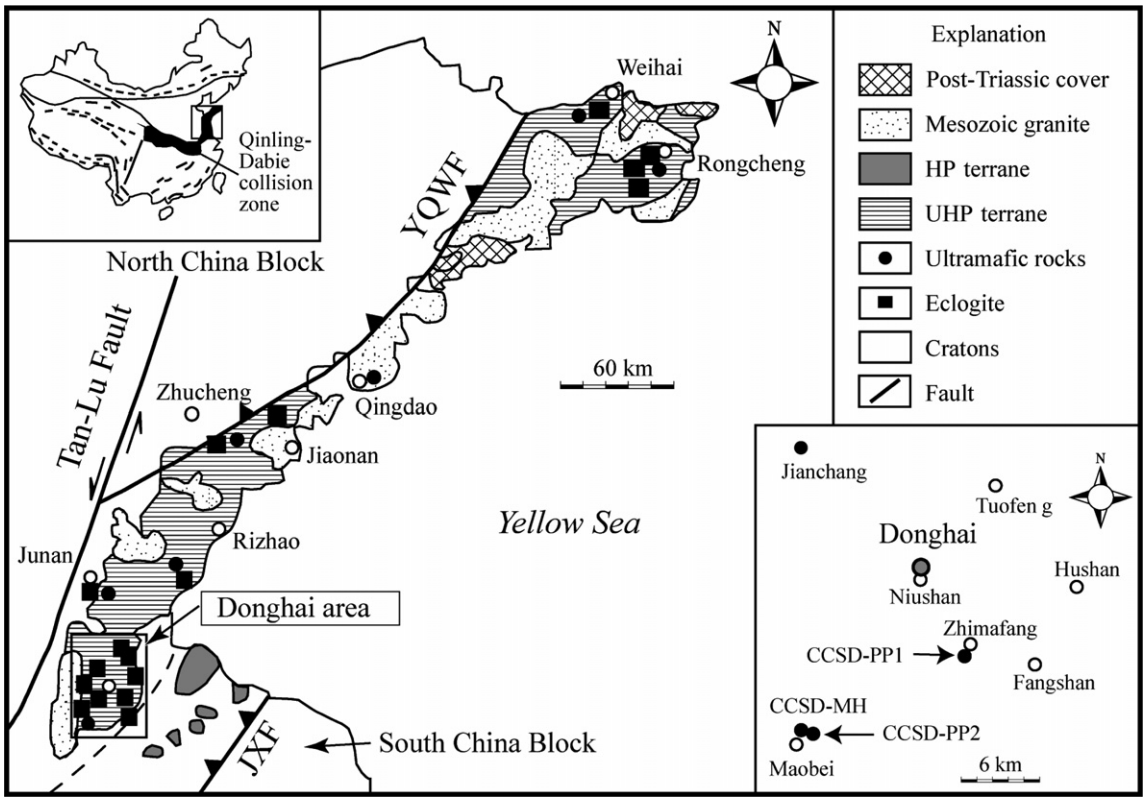

Fig. 1. Sketch map of geology in the Sulu orogen and the Donghai area, showing major lithotectonic units and locations of outcrops and pre-pilot drillhole of CCSD-PP1, CCSD-PP2 and the main hole CCSD-MH (modified after Liu et al., 2001).

CCSD-MH rocks are mainly different types of gneiss, with minor eclogite, amphibolite, peridotite, marble, schist, mylonite and cataclasite (Xu, 2004; Zhang et al., 2006a). The eclogite occurs as lenses within the gneiss, some are associated with peridotite and marble. Similar to lithological category based on field occurrence and country-rock association along the Dabie–Sulu orogenic belt (Cong, 1996; Liou et al., 1996; Zheng et al., 2003), three types of eclogite are recognized: (1) G-type, gneiss-hosted enclaves or layers; (2) M-type, interlayers with or enclaves within marble or calc-silicate rocks; (3) P-type, in association with ultramafic rocks (peridotite or pyroxenite). This study uses two continuous core segments of about 3 m length that are composed of interlayered gneiss, eclogite and amphibolite from CCSD-MH at depths of 734.21–737.16 m (Core I) and 929.67–932.86 m (Core II), respectively (Fig. 2), being named as the first and second core segments. They correspond to G-type association and thus have chemical compositions comparable to the same type of eclogite and gneiss outcropped along the Dabie–Sulu orogenic belt.

Mineral assemblages for each sample are listed in Table 1. Because mineralogical changes are significant at the contact between different lithologies, several microphotographs are presented in Fig. 3 to show these changes. Most eclogites have a mineral paragenesis of garnet + omphacite + quartz + rutile + zircon + apatite ± phengite. In some retrograded eclogites, coesite occurs as inclusion in garnet, and felsic vein crosscuts garnet grains (Fig. 3b). Textural relations and mineral paragenesis indicate that the eclogites experienced different degrees of amphibolite-facies retrogression, resulting in replacement of the primary UHP minerals by symplectite and symplectitic mineral coronas. Retrograde reactions include the formation of amphibole + plagioclase coronas after omphacite and/or garnet, replacement of omphacite and/or garnet by amphibole + plagioclase symplectites, and replacement of phengite by coronas or symplectites of plagioclase + biotite also occurs (Fig. 3b and d). Rutile is commonly rimmed by ilmenite and/or titanite. According to the modal abundance of symplectite and corona, the eclogites can be subdivided into three types (Table 1): slightly retrograde eclogite (<10%), moderately retrograde eclogite (10–30%), and highly retrograde eclogite (30–60%).

The amphibolite is generally composed of amphibole, quartz, plagioclase, garnet, biotite, epidote, apatite, zircon and rutile. Fine grained symplectite of amphibole + plagioclase after the primary omphacite and large amounts of residual garnet can be observed in the amphibolite that is close to the eclogite. In contrast, larger sizes of amphibole and plagioclase grains after omphacite and garnet, less residual garnet, more biotite and epidote occur in the amphibolite adjacent to the gneiss (Fig. 3e).

In general, the gneisses have amphibolite-facies assemblages (Table 1). The gneiss from the first core segment mainly consists of quartz, plagioclase, biotite, amphibole, garnet, epidote, with minor zircon, apatite, rutile, ilmenite and titanite. Phengite occurs in some samples, and is partly replaced by biotite + plagioclase symplectitic coronas

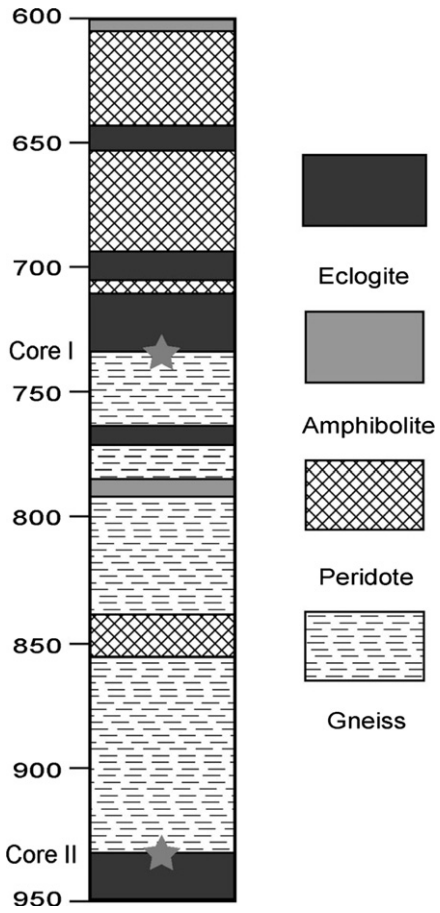

Fig. 2. Lithological profile of CCSD main hole from 600 to 950 m (revised after Zhang et al., 2006a). The core samples for this study are located at depths of 734.21–737.16 m and 929.67–932.86 m, respectively.

(Fig. 3c). The gneiss from the second core segment is composed of quartz, phengite, plagioclase, K-feldspar, biotite, apatite and zircon, with occurrence of amphibole and garnet in some samples (Table 1). Phengite is partly replaced by biotite + plagioclase symplectitic coronas (Fig. 3f).

The petrographic observations described above indicate that the primary UHP eclogite-facies minerals of the eclogites are garnet, omphacite, phengite, coesite, apatite and rutile; the amphibolite-facies retrograde metamorphism is characterized by formation of plagioclase + amphibole + biotite symplectite and/or corona after garnet, omphacite and phengite, replacement of rutile by ilmenite and/or titanite. Except for phengite and garnet, the other minerals such as quartz, feldspar, amphibole, biotite and epidote belong to amphibolite-facies assemblage in the gneisses (Zhang et al., 2000, 2006a).

3. ANALYTICAL METHODS

Whole-rock powdered samples were prepared in an agate mortar for analysis. Major element oxides and trace elements were analyzed at the Guangzhou Institute of Geochemistry, Chinese Academy of Sciences (Liu et al., 1996; Li et al., 2002). Major element analyses were done using a Varian Vista PRO ICP-AES. Trace elements were determined using a Perkin-Elmer Sciex ELAN 6000 ICP-MS. Analyses of USGS rock standards (BCR-2, BHVO-1 and AGV-1) indicate precision and accuracy better than 1% for major elements and 5% for trace elements and REE.

Whole-rock Rb–Sr and Sm–Nd isotopic analyses were made using Micromass IsoProbe MC-ICPMS at the Guangzhou Institute of Geochemistry (Liang et al., 2003). Total procedural blank of Sr is about 400 pg; analytical precisions of isotope ratio measurements are given as $\pm 2\sigma$ standard errors. Separation of Sm and Nd was done by using a routine two-column ion-exchange technique. The $^{87}Sr/^{86}Sr$ and $^{143}Nd/^{144}Nd$ ratios were normalized against $^{86}Sr/^{88}Sr = 0.1194$ and $^{146}Nd/^{144}Nd = 0.7219$. During the period of data acquisition, the Ames internal Nd standard gave $^{143}Nd/^{144}Nd$ ratios of $0.511\ 967 \pm 0.000\ 002$ (2σ), which is equivalent to the La Jolla value of 0.511 865. Initial Nd isotope ratios were calculated relative to the depleted mantle (dePaolo, 1988), but two-stage model Nd ages were calculated relative to the average continental crust (Jahn and Condie, 1995).

4. RESULTS

4.1. Major elements

Twenty eight CCSD-MH core samples were analyzed for major and trace elements (Table 2), encompassing eight granitic gneisses, three amphibolites and 17 eclogites. The eclogites show a large variation in SiO_2 content from 47.5% to 60.8% (normalized by eliminating LOI; same hereafter), with Al_2O_3 from 14.9% to 17.0%, TFe_2O_3 from 7.5% to 16.4%, MgO from 3.4% to 7.7%, CaO from 5.3% to 12.7%, and $K_2O + Na_2O$ from 1.4% to 5.7%. The samples with the same lithology from the two core segments show large differences in chemical composition. The eclogites from the first core segment, compared to those from the second core segment with similar SiO_2 contents, have relatively higher MgO and lower TiO_2 and TFe_2O_3 contents (Fig. 4). Furthermore, the eclogites form the two segments show contrasting correlations between Al_2O_3 and SiO_2, i.e. a negative correlation in the first core segment but a positive correlation in the second core segment.

A significant difference in lithochemistry occurs between the two core segments of granitic gneiss. The gneiss from the first core segment shows relatively low SiO_2 contents of 62.5–67.3% with minor variations in the contents of major and trace elements, whereas the gneiss from the second core segment exhibits relatively high SiO_2 contents of 75.2–75.9% with low contents of MgO (0.3–0.5%), TFe_2O_3 (2.0–2.5%) and CaO (1.0–1.3%). Taking the eclogites and gneisses either together or separately, SiO_2 is negatively correlated with CaO, TiO_2, TFe_2O_3 and MgO, but positively correlated with Zr (Fig. 4). These variation trends resemble those commonly observed in igneous rocks, to a first approximation, consistent with the extent of magma differentiation and/or crustal assimilation.

Significant changes in SiO_2 and K_2O concentrations occur in eclogite I5A and amphibolite II8A at the transition

Table 1
Mineral assemblages in eclogite, amphibolite and gneiss from CCSD-MH in the Sulu orogen

Sample	Depth (m)	Rock type	Mineral assemblage
Core I			
I1A	737.16	Gneiss	Qtz + Pl + Bt + Amp + Grt + Ep + Czo + Phg + Ap + Zrn + Rt + Ilm + Ttn
I2A	736.93	Gneiss	Qtz + Pl + Bt + Amp + Grt + Ep + Ap + Zrn + Rt + Ilm + Ttn
I3A	736.74	Gneiss	Qtz + Pl + Bt + Amp + Grt + Ep + Zrn + Ilm + Ttn
I4A	736.46	Gneiss	Qtz + Pl + Kfs + Bt + Amp + Grt + Phg + Ep + Ap + Zrn + Rt + Ilm + Ttn + Felsic vein
I5A	736.28	Highly retrograde eclogite	Grt + Omp + Qtz + Rt + Ttn + Zrn + Ap + Sym + Felsic vein
I6A	736.01	Moderately retrograde eclogite	Grt + Omp + Qtz + Rt + Ilm + Zrn + Ap + Sym
I7A	735.87	Highly retrograde eclogite	Grt + Omp + Phg + Bt + Qtz + Rt + Zrn + Ap + Sym + Felsic vein
I8A	735.52	Moderately retrograde eclogite	Grt + Omp + Phg + Qtz + Rt + Zrn + Ap + Sym
I9A	735.37	Slightly retrograde eclogite	Grt + Omp + Phg + Qtz + Rt + Ilm + Zrn + Ap + Sym
I10A	735.2	Highly retrograde eclogite	Grt + Omp + Phg + Qtz + Rt + Zrn + Ap + Sym
I11A	735.02	Highly retrograde eclogite	Grt + Omp + Phg + Qtz + Rt + Zrn + Ap + Sym
I12A	734.78	Slightly retrograde eclogite	Grt + Omp + Phg + Qtz + Rt + Zrn + Ap + Sym
I13A	734.39	Slightly retrograde eclogite	Grt + Omp + Qtz + Rt + Zrn + Ap + Sym
I14A	734.13	Slightly retrograde eclogite	Grt + Omp + Qtz + Rt + Ilm + Ap + Sym
Core II			
II1A	932.81	Highly retrograde eclogite	Grt + Omp + Phg + Bt + Qtz + Rt + Ilm + Zrn + Ap + Sym + Felsic vein
II1(2)A	932.49	Highly retrograde eclogite	Grt + Omp + Phg + Qtz + Rt + Zrn + Ap + Sym + Felsic vein
II2A	932.21	Moderately retrograde eclogite	Grt + Omp + Qtz + Rt + Ap + Zrn + Sym
II3A	932.03	Slightly retrograde eclogite	Grt + Omp + Phg + Qtz + Rt + Ap + Zrn + Sym
II4(1)A	931.74	Slightly retrograde Eclogite	Grt + Omp + Qtz + Rt + Ap + Zrn + Sym
II4(2)A	931.56	Slightly retrograde eclogite	Grt + Omp + Qtz + Rt + Ap + Zrn + Sym
II5A	931.33	Slightly retrograde Eclogite	Grt + Omp + Qtz + Rt + Ap + Zrn + Sym
II6A	931.11	Amphibolite	Amp + Grt + Pl + Qtz + Bt + Ep + Ap + Zrn + Rt
II7A	930.74	Amphibolite	Amp + Grt + Pl + Qtz + Bt + Ep + Ap + Zrn + Rt + Ilm + Ttn
II8A	930.52	Amphibolite	Amp + Qtz + Pl + Kfs + Ep + Grt + Bt + Zrn + Ap + Rt + Ilm
II9A	930.32	Gneiss	Qtz + Pl + Kfs + Phg + Bt + Grt + Ap + Zrn
II10A	930.16	Gneiss	Qtz + Pl + Kfs + Phg + Bt + Amp + Ap + Zrn + Mag
II11A	929.95	Gneiss	Qtz + Pl + Kfs + Phg + Bt + Ap + Zrn
II12A	929.72	Gneiss	Qtz + Pl + Kfs + Phg + Grt + Bt + Ap + Zrn

Mineral abbreviations: Amp, amphibole; Phg, phengite; Sym, symplectite (amphibole and plagioclase after omphacite and garnet), the others are after Kretz (1983).

to gneiss (Figs. 5a, b and 6a, b). Correspondingly, variable degrees of amphibolite-facies retrogression are observed for the modal abundance of minerals in the two samples (Fig. 3b and e). The similar changes in both elements and minerals also occur in eclogite I7A close to the boundary (Fig. 5a and b) and eclogites II1(2)A and II1A (Figs. 3d and 6a and b). Nevertheless, no such changes are observed in the amphibolite–eclogite transition (Fig. 6).

4.2. Trace elements

The CCSD-MH cores of both eclogite and granitic gneiss have large variations in total REE contents from 14 to 308 ppm and 125 to 296 ppm, respectively (Table 2). The eclogites has a relatively small variation in HREE contents and flat HREE distribution patterns in the chondrite-normalized REE diagrams (Fig. 7a and c). However, there is a significant variation in their LREE contents. The eclogite from the first core segment varies from pronounced LREE depletion to slight LREE enrichment with $(La/Sm)_N = 0.19–2.77$ (Table 2 and Fig. 7a). The eclogite from the second core segment also exhibits variable REE patterns from slight LREE depletion to significant LREE enrichment with $(La/Sm)_N = 0.76–4.50$ (Table 2 and Fig. 7c). While the LREE-enrichment patterns are typical for island arc basalts and continental crust, the slight LREE-depletion patterns are typical for MORB. The MORB-like REE patterns were also observed in the surface and core eclogites (especially for the high Fe–Ti eclogites) from Maobei in the Sulu orogen (Zhang et al., 2006a,b; Liu et al., 2007).

Corresponding to the difference in major elements, the granitic gneisses from the two core segments also have different REE contents and distribution patterns (Fig. 7b and d). The gneiss from the first core segment shows relatively high HREE contents and slight LREE enrichment with $(La/Sm)_N = 1.57–3.36$, whereas the gneiss from the second core segment has low HREE contents and significant LREE enrichment with $(La/Sm)_N = 4.69–5.95$ (Table 2). Compared to the eclogites, moreover, the all gneisses show considerable negative Eu anomalies with $Eu/Eu* = 0.56–0.73$.

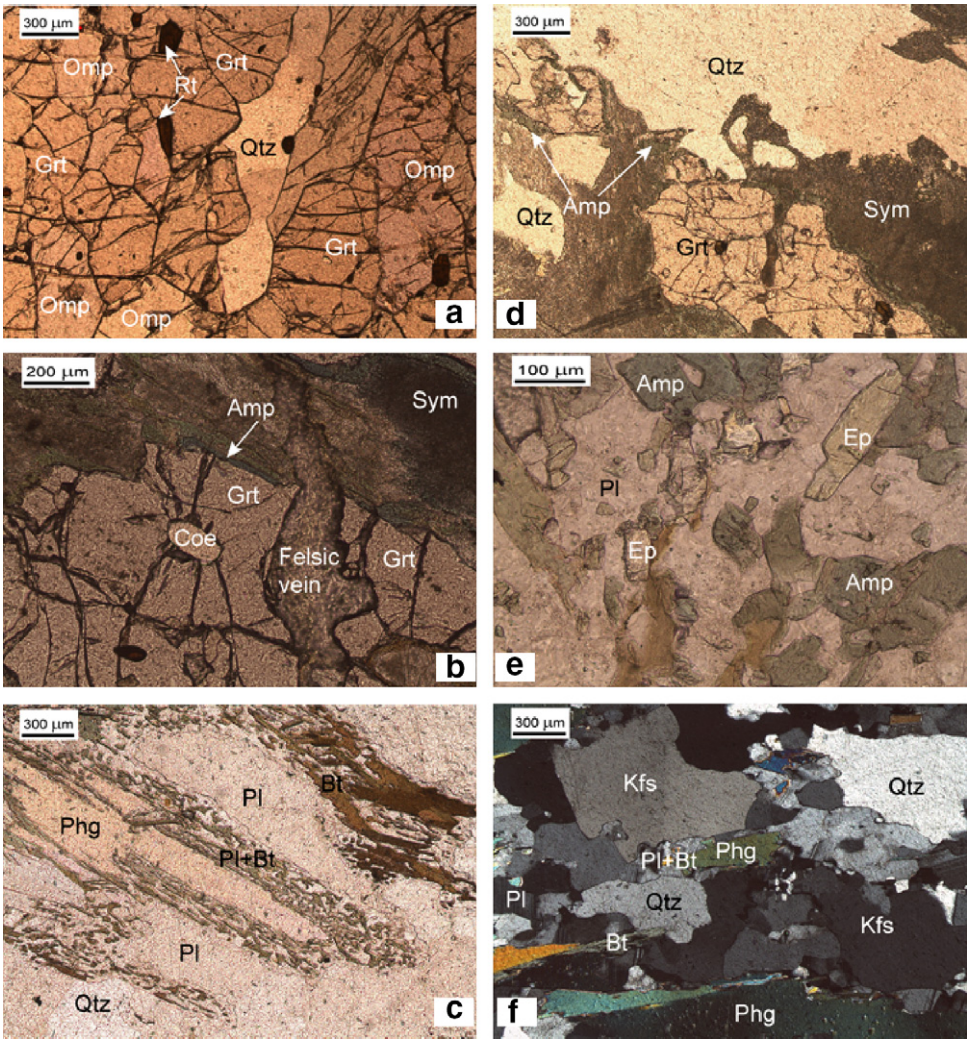

Fig. 3. Microphotographs of eclogite, gneiss and garnet amphibolite from the CCSD main hole. (a) Eclogite (I14A, 734.13 m) has an eclogite-facies mineral assemblage, composed of garnet, omphacite, quartz and rutile. (b) Retrograde eclogite (I5A, 736.28 m) with abundant symplectite primarily formed after omphacite. Coesite occurs as inclusion in garnet and felsic vein crosscuts garnet grain. (c) Gneiss (I4A, 736.46 m) contains quartz, plagioclase and biotite, with small amount of relict garnet, epidote, amphibole, apatite and zircon (not shown). Phengite is partly replaced by biotite + plagioclase symplectitic coronas. (d) Retrograde eclogite (II1A, 932.81 m) has abundant symplectite and quartz, and garnet gains are commonly rimmed by symplectite. (e) Amphibolite (II8A, 930.52 m) mainly consists of plagioclase, amphibole, epidote, with small amount of quartz, zircon, apatite biotite, and relict garnet (not shown); (f) Gneiss (II9A, 930.32 m) is mainly composed of quartz, plagioclase, K-feldspar, biotite and phengite, phengite is partly replaced by biotite + plagioclase symplectitic coronas.

In the primitive mantle-normalized spidergrams (Fig. 8a and c), the eclogites from the two core segments show significantly distinct features of trace element partitioning. Some of the eclogites are considerably depleted in LILE (e.g., Rb, Ba and K) and LREE, and the others exhibit significant enrichment of these elements relative to HFSE and HREE. Nevertheless, the all gneisses show consistently enrichment in the water-soluble elements but depletion in the water-insoluble elements and P (Fig. 8b and d). However, no good correlation is observed for Na_2O, K_2O and P_2O_5 and such LILE as Rb, Sr and Ba in both eclogite and gneiss from the two core segments. Furthermore, some of the gneisses show negative Pb anomalies (Fig. 8c and d).

Consistent increases in Rb, Ba and LREE concentrations occur in response to the changes in SiO_2 and K_2O concentrations in eclogite I5A at the transition to gneiss (Fig. 5). There are also consistent increases in Ba and LREE contents in gneisses I4A and I3A at the transition to the eclogite (Fig. 5d and e). Changes in Rb, Ba and LREE concentrations are also observed in eclogites II1(2)A and II1A (Fig. 6). At the transition to amphibolite II8A, however, gneiss II9A exhibits a decrease in LREE but gneiss II10A shows an abrupt increase in Ba content (Fig. 6). No mineralogical change is observed under the microscope for these gneiss samples (Fig. 3c and f) except occurrence of felsic veins at microscales.

4.3. Sr and Nd isotopes

Rb–Sr and Sm–Nd isotopic data for the CCSD-MH samples of eclogite and granitic gneiss are presented in Tables 3 and 4, respectively. Whole-rock $^{87}Rb/^{86}Sr$ ratios

Table 2
Major and trace element compositions of eclogite and gneiss from CCSD-MH in the Sulu orogen

Rock:	Gneiss				Eclogite									
Sample	Core I													
	I1A	I2A	I3A	I4A	I5A	I6A	I7A	I8A	I9A	I10A	I11A	I12A	I13A	I14A
Major elements (%)														
SiO_2	61.33	63.98	66.20	61.32	59.76	48.97	54.15	49.47	51.43	51.64	50.57	50.08	49.64	47.98
TiO_2	1.11	0.94	0.72	1.20	0.80	1.35	0.86	0.97	1.06	0.86	1.01	1.16	0.79	2.18
Al_2O_3	15.16	14.33	13.63	14.10	14.67	15.64	15.33	16.32	15.14	16.13	16.58	15.62	15.60	15.43
Fe_2O_3	3.20	6.82*	5.86*	8.35*	7.35*	11.59*	8.05*	2.26	2.04	1.97	1.79	1.80	2.27	2.68
FeO	4.45							7.60	7.65	6.50	7.80	8.60	7.40	10.40
MnO	0.17	0.15	0.12	0.18	0.13	0.20	0.13	0.18	0.18	0.17	0.17	0.18	0.16	0.20
MgO	2.48	2.45	2.41	2.93	4.70	7.26	6.60	7.46	6.98	7.29	7.23	7.22	7.60	6.96
CaO	4.74	4.09	3.43	4.47	5.23	10.60	8.64	11.49	10.94	10.74	10.92	11.58	12.52	11.14
Na_2O	3.14	3.62	3.26	3.20	3.03	3.17	3.05	2.11	1.97	2.11	1.93	2.09	2.90	1.33
K_2O	1.90	2.01	2.63	2.28	2.55	0.22	1.63	0.66	0.57	1.06	0.81	0.27	0.10	0.07
P_2O_5	0.27	0.22	0.16	0.13	0.09	0.08	0.14	0.04	0.17	0.13	0.06	0.06	0.03	0.05
LOI	1.79	0.67	0.90	1.21	1.09	0.63	0.98	1.23	1.18	1.12	0.90	0.61	0.80	0.58
Total	99.74	99.28	99.32	99.37	99.40	99.71	99.56	99.79	99.31	99.72	99.77	99.27	99.81	99.00
Mg#	40	44	48	44	58	58	64	61	59	64	60	58	61	52
Trace elements (ppm)														
Ba	535	511	1094	1201	838	758	1196	164	301	816	259	70.1	47.0	16.3
Rb	55.9	53.4	69.1	57.5	65.1	5.01	29.8	13.7	13.0	26.1	17.9	6.23	2.82	1.74
Sr	202	138	154	282	187	316	259	92.2	130	236	87.9	68.3	82.3	44.4
Ta	0.470	0.541	0.494	0.606	0.231	0.171	0.206	0.128	0.141	0.129	0.124	0.145	0.118	0.101
Nb	8.26	9.84	8.62	10.9	3.80	3.14	3.97	1.61	2.13	1.72	2.01	1.95	1.89	1.64
Hf	5.50	7.39	7.93	6.26	6.19	2.41	3.87	1.29	2.88	2.30	3.22	2.41	1.84	1.32
Zr	229	278	305	242	281	91.9	154	38.7	101	79.0	114	93.8	57.4	39.4
Th	3.51	2.94	4.54	7.11	1.70	1.83	0.349	1.04	0.520	0.500	0.480	0.633	0.300	0.116
U	0.970	0.744	1.00	1.18	0.645	0.497	0.369	0.472	0.310	0.160	0.170	0.427	0.050	0.178
Cr	24.3	39.6	45.4	35.0	94.1	171	160	213	208	190	209	182	209	140
Ni	15.9	23.3	32.3	21.3	68.4	81.9	118	126	114	129	123	97.2	123	79.5
Sc	24.9	22.9	19.6	28.9	26.7	44.9	31.7	33.7	42.5	37.5	36.6	37.3	41.3	45.3
V	154	131	100	148	149	306	197	201	282	231	260	270	468	406
Pb	3.80	2.60	4.70	6.20	7.29	6.37	7.62	5.00	5.10	8.80	5.00	3.45	1.50	2.57
Co	18.8	17.5	17.2	21.0	33.4	37.5	41.9	42.9	50.0	40.5	46.3	41.6	44.3	58.3
Ga	20.4	18.8	19.2	18.7	17.4	18.1	18.4	14.4	15.4	17.0	16.0	15.8	19.9	15.3
Y	48.8	55.8	51.1	61.9	29.2	27.7	26.2	19.4	21.9	23.8	19.4	19.5	19.4	19.7
REE (ppm)														
La	18.1	17.8	30.0	46.6	18.6	13.1	5.73	17.8	3.65	2.12	1.45	12.3	0.426	0.446
Ce	37.5	38.3	62.4	96.2	36.7	29.8	15.4	34.9	9.17	5.86	3.82	26.8	0.974	1.28
Pr	5.76	5.21	8.28	12.4	4.80	4.12	2.25	4.15	1.56	0.936	0.576	3.36	0.236	0.256
Nd	26.4	22.8	32.5	46.8	20.3	17.8	10.5	18.2	7.34	4.49	3.39	15.2	1.34	1.66
Sm	7.22	6.09	6.64	8.67	4.20	4.41	3.58	4.02	3.08	2.13	2.11	3.28	1.32	1.45
Eu	2.01	1.53	1.46	1.87	1.18	1.42	1.26	1.20	1.22	0.904	0.962	1.11	0.782	0.931
Gd	9.83	7.77	6.74	7.58	4.47	5.33	4.36	3.64	3.92	2.95	3.14	3.29	2.24	2.64

Tb	1.66	1.40	1.21	1.44	0.801	0.908	0.718	0.639	0.681	0.552	0.571	0.628	0.421	0.492
Dy	10.0	8.65	7.82	9.07	5.18	5.25	4.59	3.61	4.33	3.55	3.81	3.62	2.64	3.04
Ho	1.88	1.88	1.65	1.90	1.16	1.04	1.01	0.788	0.872	0.731	0.773	0.795	0.520	0.612
Er	5.16	5.27	4.74	5.63	3.36	2.74	2.88	2.20	2.66	2.18	2.34	2.23	1.41	1.63
Tm	0.770	0.893	0.842	0.989	0.557	0.408	0.481	0.329	0.421	0.343	0.371	0.332	0.220	0.242
Yb	4.80	6.05	5.74	6.45	3.79	2.62	3.20	2.02	2.74	2.22	2.36	2.05	1.31	1.42
Lu	0.710	0.940	0.899	0.981	0.610	0.397	0.506	0.294	0.402	0.334	0.362	0.299	0.203	0.213
ΣREE	132	125	171	247	106	89.3	56.5	93.8	42.0	29.3	26.0	75.3	14.0	16.3
$(La/Sm)_N$	1.57	1.83	2.82	3.36	2.77	1.86	1.00	2.77	0.74	0.62	0.43	2.34	0.20	0.19

Rock:	Eclogite							Amphibolite			Gneiss			
Sample	Core II													
	II1A	II1(2)A	II2A	II3A	II4(1)A	II4(2)A	II5A	II6A	II7A	II8A	II9A	II10A	II11A	II12A
Major elements (%)														
SiO_2	53.09	53.00	46.78	48.12	46.83	48.02	47.13	47.30	46.93	56.58	74.09	73.93	74.55	73.81
TiO_2	1.38	1.53	2.18	1.62	1.80	2.36	1.79	1.84	1.80	1.12	0.31	0.48	0.46	0.33
Al_2O_3	16.58	16.31	15.29	15.63	15.52	15.11	15.43	15.03	15.30	16.62	14.18	13.33	13.87	13.89
Fe_2O_3	2.64	11.94*	15.72*	2.85	2.50	16.29*	3.67	4.18	5.44	8.96*	1.92*	1.02	1.28	2.21*
FeO	7.50			10.30	11.70		11.20	10.00	8.90			1.25	1.02	
MnO	0.18	0.16	0.23	0.21	0.23	0.25	0.24	0.23	0.25	0.17	0.04	0.06	0.06	0.05
MgO	4.50	3.79	5.92	6.05	6.43	5.79	6.00	6.33	6.19	3.39	0.36	0.48	0.46	0.28
CaO	7.03	8.70	10.13	10.69	11.02	9.49	10.50	10.64	10.00	5.87	0.97	1.29	1.13	1.14
Na_2O	2.47	1.85	2.08	2.16	2.03	1.93	2.26	0.90	1.86	2.93	3.44	3.70	4.17	4.21
K_2O	1.85	1.14	0.04	0.59	0.18	0.03	0.13	0.48	0.67	2.49	2.34	2.58	1.60	2.21
P_2O_5	0.27	0.48	0.22	0.21	0.22	0.29	0.22	0.22	0.27	0.30	0.03	0.10	0.08	0.03
LOI	2.24	0.70	1.20	0.67	0.63	0.17	0.54	1.91	2.17	1.05	1.32	1.19	0.94	1.16
Total	99.73	99.60	99.79	99.10	99.09	99.73	99.11	99.06	99.78	99.48	99.00	99.41	99.62	99.32
Mg#	47	41	45	48	48	44	45	48	47	45	29	30	30	22
Trace elements (ppm)														
Ba	752	461	3.88	183	97.5	33.1	83.7	359	191	708	1148	3943	2025	2194
Rb	42.7	24.3	0.344	13.3	4.99	0.478	3.47	12.1	10.6	52.9	42.3	39.8	30.9	43.6
Sr	240	229	115	154	160	171	151	438	205	151	285	593	361	404
Ta	0.320	0.385	0.161	0.124	0.110	0.182	0.129	0.130	0.143	0.361	0.671	0.601	0.650	0.626
Nb	5.06	5.88	2.65	1.89	1.88	2.98	1.92	2.07	2.40	6.29	12.4	11.4	12.2	11.2
Hf	4.30	3.11	2.15	2.02	2.90	3.00	2.24	3.00	2.27	5.50	8.17	9.50	10.4	7.85
Zr	195	145	85.9	76.3	87.9	121	80.6	94.5	81.4	234	315	289	326	305
Th	2.31	3.03	0.227	0.340	0.580	0.439	0.386	0.519	0.580	2.76	8.07	8.71	6.33	11.0
U	0.59	0.68	0.114	0.174	0.201	0.187	0.173	0.191	0.226	0.548	1.09	1.22	1.17	1.60
Cr	111	137	66.8	111	126	53.4	98.9	120	106	50.0	3.69	5.62	1.18	3.53
Ni	57.8	74.7	51.6	73.4	72.1	37.6	61.8	72.7	66.7	24.4	1.11	3.01	1.82	2.13
Sc	29.0	29.9	57.8	36.2	49.2	54.8	40.2	43.3	36.9	27.2	5.42	6.58	6.43	7.59
V	206	243	472	327	492	487	354	448	309	176	19.9	31.9	21.0	18.2
Pb	4.90	6.46	2.11	3.52	3.90	2.24	2.88	2.70	3.49	4.02	7.10	22.6	4.80	5.90
Co	36.1	45.2	53.2	46.1	52.2	53.8	46.3	48.2	46.2	26.2	1.43	2.47	1.42	1.88
Ga	18.2	20.3	19.3	18.0	19.9	21.2	18.2	18.0	16.8	19.1	16.3	15.5	16.4	17.1
Y	25.4	30.1	29.70	27.2	26.4	36.4	28.6	28.7	32.1	37.2	15.5	22.7	24.6	28.4

(*continued on next page*)

Table 2 (*continued*)

Rock:	Eclogite						Amphibolite			Gneiss			
Sample	Core II												
	II1A	II1(2)A	II2A	II3A	II4(1)A	II4(2)A	II5A	II6A	II7A	II8A	II9A	II10A	II11A	II12A
REE (ppm)														
La	58.3	64.9	4.23	5.12	18.0	6.58	4.00	8.00	7.59	31.7	36.9	65.5	71.8	64.0
Ce	107	128	11.5	14.7	41.4	17.0	11.1	18.8	20.4	65.2	66.9	105	122	112
Pr	13.6	16.4	2.12	2.40	6.56	3.05	1.85	3.14	3.09	8.46	7.76	13.1	15.8	12.9
Nd	49.8	62.7	10.5	13.0	26.0	16.1	9.24	14.5	15.9	34.0	25.5	44.0	54.8	46.2
Sm	8.09	10.8	3.42	3.98	5.69	4.66	3.29	4.34	4.55	6.69	4.18	6.87	9.21	8.53
Eu	2.51	3.31	1.43	1.47	2.07	1.79	1.38	1.76	1.66	1.88	0.63	1.37	1.84	1.37
Gd	6.08	7.70	4.84	4.51	5.52	5.84	4.51	5.24	5.26	5.95	2.76	4.75	6.77	6.46
Tb	0.960	1.09	0.868	0.827	0.928	1.04	0.881	0.948	1.02	1.02	0.428	0.731	0.941	1.00
Dy	5.33	5.58	5.36	4.82	5.59	6.48	5.13	5.90	5.94	5.86	2.54	4.28	5.08	5.26
Ho	1.11	1.07	1.11	1.06	1.10	1.36	1.12	1.17	1.28	1.22	0.507	0.962	1.04	0.911
Er	2.98	2.95	3.00	2.97	3.07	3.67	3.10	3.21	3.52	3.31	1.65	3.32	2.89	2.47
Tm	0.490	0.417	0.452	0.439	0.481	0.564	0.449	0.511	0.508	0.548	0.288	0.633	0.482	0.396
Yb	2.89	2.73	2.90	2.62	2.83	3.62	2.78	3.05	3.11	3.67	1.91	4.41	3.06	2.79
Lu	0.460	0.422	0.442	0.377	0.439	0.546	0.389	0.462	0.434	0.534	0.365	0.752	0.493	0.411
ΣREE	260	308	52.2	58.3	120	72.3	49.2	71.0	74.3	170	152	256	296	265
$(La/Sm)_N$	4.50	3.75	0.77	0.80	1.98	0.88	0.76	1.15	1.04	2.96	5.51	5.95	4.87	4.69

*Total iron as Fe_2O_3; Mg#, molecular proportion of MgO/(MgO + FeO), assuming 90% of total iron oxides as FeO.

for the eclogite and gneiss are relatively low, but have a large variation from 0.008 to 1.29. Calculated initial $^{87}Sr/^{86}Sr$ ratios are 0.7058–0.7095 at $t = 220$ Ma, but some samples exhibit unreasonably low ratios of 0.6986–0.7019 when calculated at $t = 750$ Ma. This indicates that their Rb–Sr isotopic system suffered secondary disturbance (Zheng, 1989), which may occur during subduction-zone metamorphism at the Triassic. Eclogite II4(2)A has relatively high $^{87}Sr/^{86}Sr$ ratio of 0.7069 but very low Rb content of 0.48 ppm (Table 3). The similar case was also encountered in the eclogites outcropped in the Dabie–Sulu orogenic belt (Jahn, 1998; Chen et al., 2002), where Rb is extremely depleted relative to Sr.

Whole-rock $^{147}Sm/^{144}Nd$ ratios for the eclogite and gneiss are 0.0988–0.5969 (Table 4). Some eclogites from the first core segment have very high $^{147}Sm/^{144}Nd$ ratios of 0.3758 to 0.5969, resulting in unreasonably low $\varepsilon_{Nd}(t)$ values of −30.3 to −12.4 at $t_1 = 750$ Ma but reasonable $\varepsilon_{Nd}(t)$ values of −3.1 to −0.2 at $t_2 = 220$ Ma in comparison to the other eclogites. Both eclogite and gneiss from the first core segment have relatively high $\varepsilon_{Nd}(t)$ values of −6.0 to −0.2 at $t_2 = 220$ Ma with young Nd model ages of 1.44–1.72 Ga, whereas those from the second core segment have low $\varepsilon_{Nd}(t)$ values of −15.1 to −10.7 at $t_2 = 220$ Ma with old Nd model ages of 1.87–2.22 Ga. It appears that the second core segment is more enriched than the first core segment with respect to their protolith nature and thus more components of ancient crust were involved in the former relative to the latter.

5. DISCUSSION

While the oceanic subduction-zone metamorphism is associated with the coupling or decoupling between dehydration and loss of water-soluble elements, it is of great interest how elements behave during the continental subduction-zone metamorphism. Many previous studies have demonstrated that the oceanic subduction-zone metamorphism is not an isochemical process, resulting in large variations in the contents of water-soluble elements. Abundant aqueous fluid is released when transforming the altered oceanic basalt and overlying sediment to eclogite-facies assemblages during deep subduction (e.g., Rüpke et al., 2002). In association with the release of fluid, large amounts of water-soluble elements are lost from the water-rich oceanic crust (e.g., Arculus et al., 1999; Becker et al., 2000; Polat et al., 2002; John et al., 2004). Such a fluid enriching some LILE and LREE is assumed to metasomatize the overlying mantle wedge, resulting in syn-subduction island-arc magmatism (e.g., Hawkesworth et al., 1991; Tatsumi and Eggins, 1995).

In contrast, the continental crust is principally composed of crystalline basement and overlying sedimentary rocks that were poor of water prior to subduction (Liou et al., 1997; Fu et al., 2001; Zheng et al., 2003). During subduction, only limited amounts of water would be redistributed within the HP–UHP slabs as hydrous minerals, molecular water (fluid inclusions) and structural hydroxyl incorporating into nominally anhydrous minerals. Thus no sufficient fluid was available for release to cause arc-type

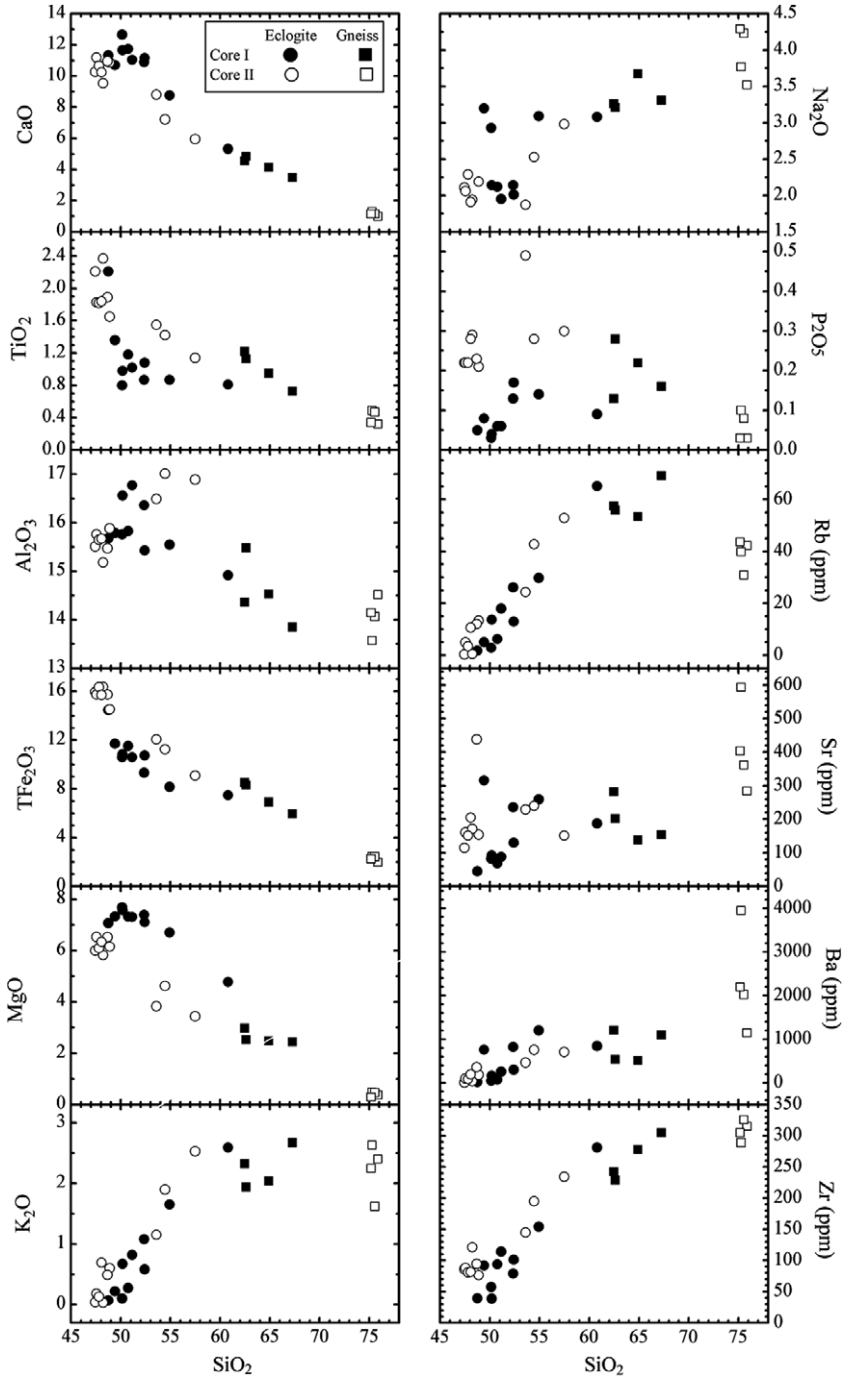

Fig. 4. Plots of major and selected trace elements vs. SiO_2 for eclogite and gneiss from CCSD-MH.

magmatism. However, the decomposition of hydrous minerals and the exsolution of structural hydroxyl and molecular water from nominally anhydrous minerals would take place due to a profound decrease in pressure during exhumation (Zheng et al., 1999, 2003; Li et al., 2001, 2004; Xia et al., 2005; Chen et al., 2007a; Sheng et al., 2007; Zhao et al., 2007), capable of resulting in syn-exhumation magmatism, quartz veining and widespread amphibolite-facies retrogression. Therefore, it is important to understand the geochemical behavior of elements during the continental subduction-zone metamorphism.

Previous studies compared HP–UHP eclogites with MORB and OIB that did not suffer high-grade metamorphism when discussing the geochemical behavior of elements during the oceanic subduction-zone metamorphism (e.g., Arculus et al., 1999; Becker et al., 2000; John et al., 2004). This approach cannot be directly applied to the HP-UHP metamorphic products of continental crust

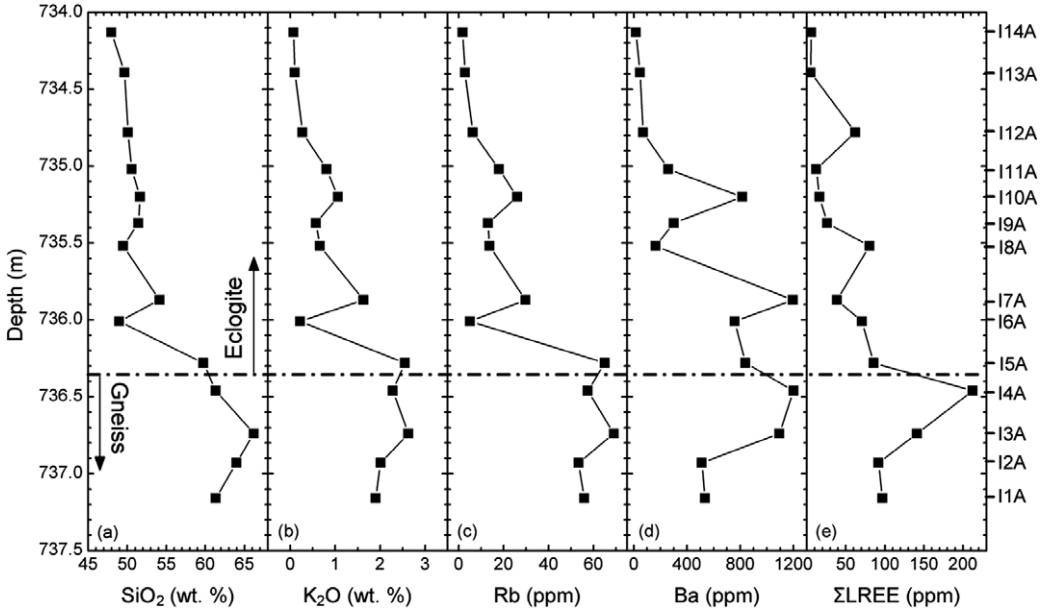

Fig. 5. Profiles of SiO_2, Rb, Ba, K_2O and LREE (La to Eu) contents of the eclogite and gneiss from the first core segment.

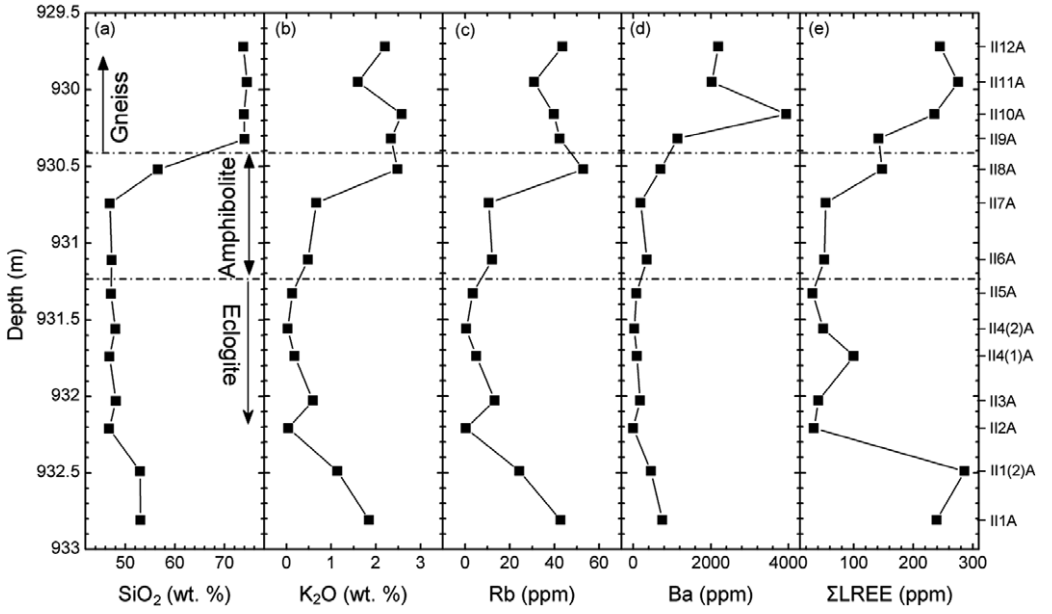

Fig. 6. Profiles of SiO_2, Rb, Ba, K_2O and LREE (La to Eu) contents of the eclogite, amphibolite and gneiss from the second core segment.

because of significant variations in the element and isotope compositions of premetamorphic protolith. Nevertheless, numerous geochemical studies have established that protolith of Dabie–Sulu UHP eclogites is continental basaltic and/or gabbroic rocks (e.g., Jahn et al., 2003). Furthermore, a large number of zircon U–Pb dates are now available by both TIMS, SIMS and LA-ICPMS methods for Dabie–Sulu UHP metaigneous rocks, mostly yielding protolith ages of 740–820 Ma with a cluster at about 750 Ma (e.g., Ames et al., 1996; Hacker et al., 1998; Zheng et al., 2003, 2004, 2006; Tang et al., 2007b). The similar ages have also been obtained by the SHRIMP zircon U–Pb dating for the UHP metamorphic rocks from the CCSD pilot and main holes (Liu et al., 2004a,b, 2005; Liu and Xu, 2004; Zhang et al., 2006b). Therefore, protoliths of both eclogite and granitic gneiss from this study are reasonably assumed to result from bimodal magmatism in a rift tectonic zone during the middle Neoproterozoic (Zheng et al., 2004, 2006).

While the granitic gneiss from the same CCSD core segment exhibits relatively limited variations in both major and trace elements, the eclogite and amphibolite show large variations in both major and trace element compositions (Table 2 and Fig. 4). In particular, some trace elements such as LILE and LREE appear to have significantly distinct

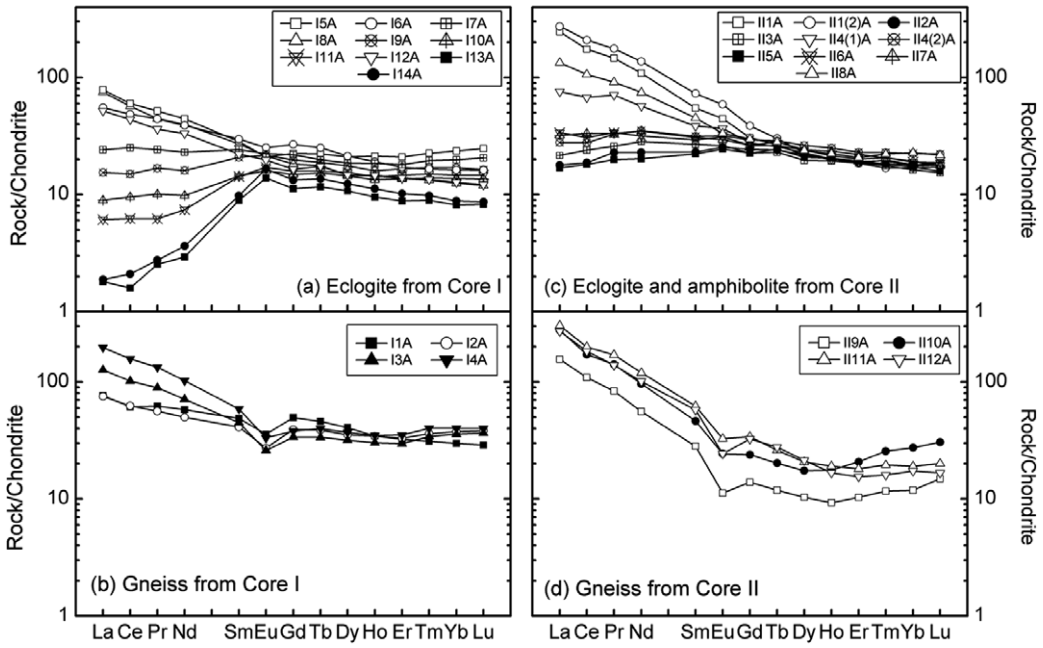

Fig. 7. Plots of chondrite-normalized REE patters for eclogite (a, c) and gneiss (b, d) from CCSD-MH. Chondrite values are from McDonough and Sun (1995).

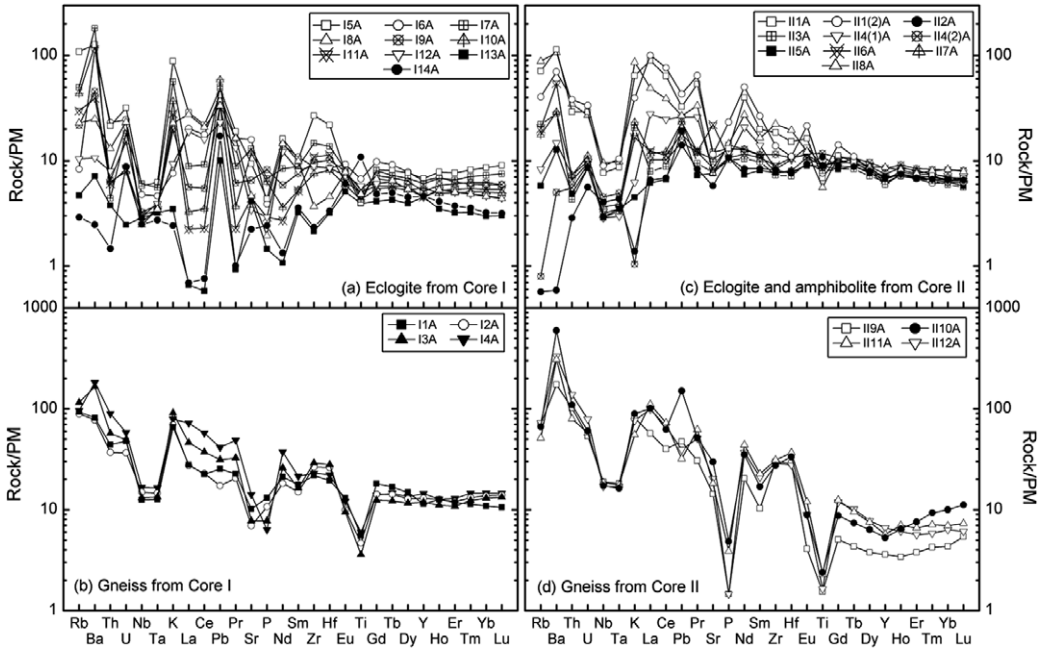

Fig. 8. Primitive mantle-normalized spidergrams for eclogite (a, c) and gneiss (b, d) from CCSD-MH. Primitive mantle values are from McDonough and Sun (1995).

features of abundance distribution (Figs. 7a and c, and 8a and c). This can be caused by either protolith heterogeneity or geochemical modification during high-grade metamorphism (e.g., Jahn et al., 2003; John et al., 2004). For eclogites I13A and I14A, in particular, they show positive Eu anomalies that are usually used to indicate cumulus plagioclase in igneous protolith. Also the overall shape of their REE patterns is similar to plagioclase–pyroxene cumulus dominated rocks. Thus the depletion of LREE and LILE in these two samples could be inherited from the mafic protolith that was derived from gabbro rather than basalt. The wholly observed variation in REE in the first core segment could be explained by the protolith variations: (1) the cumulus dominated mafic rocks have low LREE, (2) the melt dominated mafic rocks have the high LREE, and (3) mixed members plot in between.

Table 3
Whole-rock Rb–Sr isotopic compositions of eclogite and gneiss from CCSD-MH in the Sulu orogen

Sample	Rock	Rb (ppm)	Sr (ppm)	$^{87}Rb/^{86}Sr$	$^{87}Sr/^{86}Sr$	I_{Sr} (t_2) $t_2 = 220$ Ma	$I_{Sr}(t_1)$ $t_1 = 750$ Ma
Core I							
I5A	Eclogite	65.13	186.7	1.0065	0.711235	0.7081	0.7005
I7A	Eclogite	29.82	258.7	0.4454	0.708811	0.7074	0.7040
I9A	Eclogite	13.00	129.6	0.2903	0.707833	0.7069	0.7047
I11A	Eclogite	17.92	87.9	0.5901	0.708200	0.7064	0.7019
I13A	Eclogite	2.82	82.3	0.0991	0.706131	0.7058	0.7051
I14A	Eclogite	1.74	44.4	0.1134	0.706266	0.7059	0.7051
I2A	Gneiss	53.44	138.2	1.1158	0.712269	0.7088	0.7003
I3A	Gneiss	69.08	154.3	1.2918	0.712481	0.7084	0.6986
Core II							
II1(2)A	Eclogite	24.31	229.3	0.3068	0.708460	0.7075	0.7052
II4(2)A	Eclogite	0.48	171.1	0.0080	0.706962	0.7069	0.7069
II8A	Amphibolite	52.92	151.0	1.0145	0.710597	0.7074	0.6997
II9A	Gneiss	42.30	284.7	0.4299	0.710187	0.7088	0.7056
II12A	Gneiss	43.59	404.1	0.3112	0.710426	0.7095	0.7071

Table 4
Whole-rock Sm–Nd isotopic compositions of eclogite and gneiss from CCSD-MH in the Sulu orogen

Sample	Rock	Sm (ppm)	Nd (ppm)	$\frac{^{147}Sm}{^{144}Nd}$	$\frac{^{143}Nd}{^{144}Nd}$	$\varepsilon_{Nd}(t_2)$	$\varepsilon_{Nd}(t_1)$	T_{DM} (Ga)	T_{DM2} (Ga)	
									t_2	t_1
Core I										
I5A	Eclogite	4.20	20.28	0.1252	0.512312	−4.4	0.5	1.44		
I7A	Eclogite	3.58	10.48	0.2066	0.512473	−3.5	−4.2			
I9A	Eclogite	3.08	7.34	0.2535	0.512571	−2.9	−6.8			
I11A	Eclogite	2.11	3.39	0.3758	0.512884	−0.2	−12.4			
I13A	Eclogite	1.32	1.34	0.5969	0.513056	−3.1	−30.3			
I14A	Eclogite	1.45	1.66	0.5254	0.513062	−1.0	−23.3			
I2A	Gneiss	6.09	22.8	0.1615	0.512281	−6.0	−3.6		1.48	1.72
I3A	Gneiss	6.64	32.53	0.1234	0.512241	−5.7	−0.7	1.53	1.46	1.49
Core II										
II1(2)A	Eclogite	10.81	62.73	0.1042	0.511803	−13.7	−7.4	1.87		
II4(2)A	Eclogite	4.66	16.11	0.1749	0.512053	−10.8	−9.3			
II8A	Amphibolite	6.69	34.03	0.1189	0.511976	−10.7	−5.5	1.88		
II9A	Gneiss	4.18	25.54	0.0988	0.511724	−15.1	−8.5	1.89	2.22	2.11
II12A	Gneiss	8.53	46.15	0.1117	0.511777	−14.4	−8.7	2.04	2.16	2.13

Two-stage Nd model ages (T_{DM2}) were calculated relative to the average continental crust at $t_2 = 220$ Ma and $t_1 = 750$ Ma, respectively.

For a given core segment, the most pronounced compositional variations occur in eclogites I5A, I7A, II1A, II1(2)A and amphibolite II8A. They have andesitic compositions as reflected by higher contents of SiO_2 (53.6–60.8%) and alkali ($Na_2O + K_2O$, 3.0–5.7%) but lower contents of CaO (5.3–8.8%), MgO (3.4–6.7%) and total Fe_2O_3 (7.5–12.1%) compared to the other eclogites and amphibolites from the same core segment (Table 2 and Fig. 4). If these features would result from magma differentiation and/or crustal assimilation during igneous process of their protolith formation in the Neoproterozoic, significantly low Mg# numbers should be expected for these samples. However, their Mg# numbers are similar to those for the other eclogites and/or amphibolites from the same core segment (Table 2). This suggests that the large variations in composition of the eclogite and amphibolite are not related to their protolith heterogeneity, but caused by geochemical modification during the subduction-zone metamorphism. The similar case was also observed from the eclogites at Weihai in the eastern end of the Sulu orogen, where high SiO_2 contents of 54–60% for the eclogites are demonstrably of metasomatic origin (Jahn et al., 1996).

The Triassic metamorphic modification is also supported by Rb–Sr and Sm–Nd isotopic systematics in the UHP metamorphic rocks. As shown in Table 3 and Fig. 9, some samples show unreasonably low initial $^{87}Sr/^{86}Sr$ ratios of 0.6986–0.7019 at $t = 750$ Ma (protolith age) but reasonable initial$^{87}Sr/^{86}Sr$ ratios of 0.7074–0.7088 at $t = 220$ Ma (metamorphism age). The eclogites show various REE distribution patterns with LREE enrichment and depletion (Fig. 7a and c). In particular, the strong LREE depletion is remarkable for eclogites I13A and I14A, which have very high $^{147}Sm/^{144}Nd$ ratios of 0.5254–0.5969 and unreasonably low $\varepsilon_{Nd}(t)$ value of −30.3 to −23.3 at $t = 750$ Ma (protolith age) but reasonable $\varepsilon_{Nd}(t)$ values of −3.1 to −1.0 at $t = 220$ Ma (metamorphism age) compared to the other eclogites from the first core segment (Table 4 and Fig. 9). These point to the metamorphic modification that results in removal of both water-soluble and -insoluble elements in association with fluid/melt metasomatism.

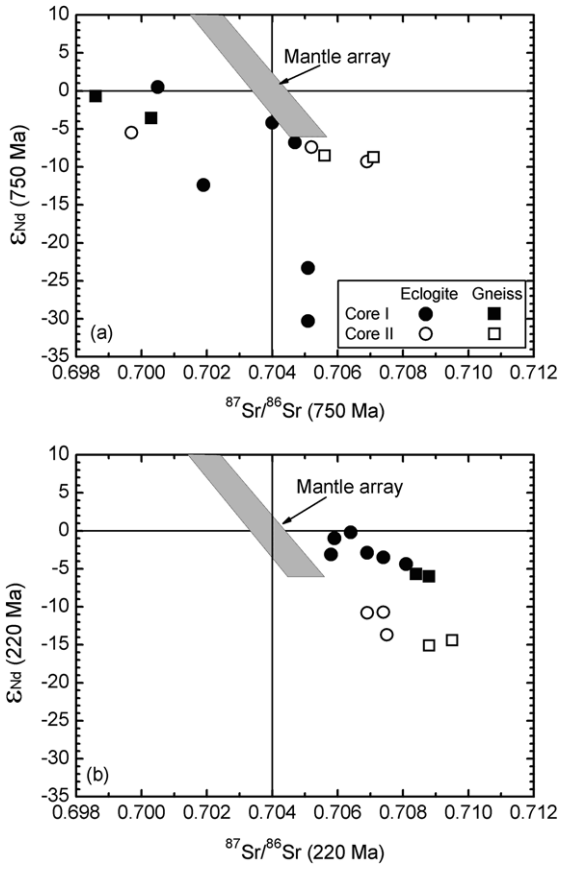

Fig. 9. Plots of the initial Sr and Nd isotope ratios at $t_1 = 750$ Ma (a) and $t_2 = 220$ Ma (b) for eclogite and gneiss from CCSD-MH.

Collectively, all the observations noted above indicate that the large variations of some elements in the UHP metamorphic rocks from the two CCSD core segments are unlikely caused by the protolith heterogeneity, but by the geochemical modification during the Triassic subduction-zone metamorphism. The element mobility could take place in the stages of prograde and/or retrograde metamorphism in association with fluid and/or melt availability during subduction and exhumation of the continental crust (Li et al., 2004; Zheng et al., 2005b; Auzanneau et al., 2006; Hermann et al., 2006; Wu et al., 2006a; Xiao et al., 2006a; Spandler et al., 2007). In this regard, it is critical to have distinction between the fluid and melt effects on the mobility of different elements during the continental collision and to identify the occurrence of partial melts in the UHP rocks.

6. ELEMENT MOBILITY DURING CONTINENTAL COLLISION

6.1. Fluid-induced element mobility

Trace element liberation accompanying mineral dehydration is often invoked to explain the distinctive enrichment of LILE and LREE relative to HFSE found in arc magmas (e.g., Tatsumi and Eggins, 1995; Kogiso et al., 1997; Becker et al., 2000; John et al., 2004; Zack and John, 2007). However, recent studies indicate that devolatilisation associated with eclogite-facies metamorphism may not result in significant chemical alteration of the resultant metamorphic rocks, implying that fluids released during the oceanic subduction-zone metamorphism contained low solute contents (e.g., Chalot-Prat et al., 2003; Spandler et al., 2003, 2004). Trace elements were not liberated in significant quantities by prograde metamorphism up to eclogite-facies, but retained by newly-formed major and accessory minerals during breakdown reactions (Spandler et al., 2003). For example, from blueschist- to eclogite-facies, phengite is a major host of LILE (e.g., Becker et al., 2000; Zack et al., 2001), lawsonite and epidote-group are the main minerals containing LREE in metabasic and metapelitic rocks (Tribuzio et al., 1996; Zack et al., 2002). Experimental studies of accessory mineral stability show that allanite is present as a breakdown product of zoisite, with almost more than 90% of bulk LREE and Th, and 70–80% of U to be redistributed into the allanite (Hermann, 2002a).

In contrast, Breeding et al. (2004) and John et al. (2004) document significant removal of such trace elements as LILE and LREE from blueschist- and eclogite-facies rocks in zones of channeled fluid flow. In these cases, element removal was most probably achieved through prolonged low-level dissolution at high fluid/rock ratios, rather than through high element solubilities in the fluid (Hermann et al., 2006; Spandler et al., 2007). The experimental study of Stalder et al. (1998) for trace element partition between aqueous fluid and eclogite minerals (garnet, clinopyroxene, and rutile) at 900–1200 °C and 3.0–5.7 GPa indicates that in the presence of garnet or clinopyroxene, Nb and Ta are highly soluble in aqueous fluids, whereas Zr and Hf show variable solubilities. Furthermore, high solubilities of trace elements may occur in the supercritical fluid that has no immiscibility gap between aqueous fluid and hydrous melt. This is documented by experimental studies of Kessel et al. (2005a,b) that show concomitant increases of SiO_2 and LILE in the supercritical fluids equilibrated with basaltic eclogite under P–T conditions of subduction zones. Ferrando et al. (2005) found very high amounts of elements Si, Al and Ti, in the order of tens of wt%, in fluids of multiphase solid inclusions within primary garnet and kyanite from UHP eclogite at Donghai, revealing the possible presence of supercritical fluid during UHP eclogite-facies metamorphism.

Anomalously low $\delta^{18}O$ values of −11‰ to −2‰ were observed for zircon and other minerals from UHP eclogite and gneiss in the Dabie–Sulu orogenic belt (Rumble et al., 2002, 2003; Zheng et al., 2003, 2004; Tang et al., 2007b), indicating that their protoliths experienced high-T meteoric-hydrothermal alteration and even low $\delta^{18}O$ magmatism. The ^{18}O-depletion is also observed in the CCSD-MH eclogite and gneiss from this study, with garnet $\delta^{18}O$ values of −7.4‰ to 7.5‰ (Xiao et al., 2006b; Chen et al., 2007b; Zhao et al., 2007). However, the continental crust is less hydrated compared to the oceanic crust, especially in the lower crust which is composed mainly of granulite-facies rocks containing no hydrous minerals. Therefore, significant fluid activity and element mobility are unlikely to

occur during subduction of the lower crust although it can contain significant amounts of structural hydroxyl in nominally anhydrous minerals (Xia et al., 2006).

On the other hand, fluid activity during exhumation of the deeply subducted continental crust is evidenced by different degrees of amphibolite-facies retrogression in the UHP metamorphic rocks (Table 1 and Fig. 3). Mineral O isotope studies of UHP metamorphic rocks from the Dabie–Sulu orogenic belt indicate that the amphibolite-facies retrogression caused mineral reactions and O isotope disequilibria between some of the minerals (Zheng et al., 1999, 2003; Zhang et al., 2003; Li et al., 2004). Considerable changes occur in $\delta^{18}O$ and petrography at the contact between eclogite and gneiss in the CCSD-MH core samples (Chen et al., 2007b), suggesting that the contact between different lithologies is the most favorable place for fluid activity. The stable isotope studies have demonstrated that the retrograde fluid is of deuteric origin and thus was derived from the decompression exsolution of structural hydroxyl and molecular water (Zheng et al., 1999, 2003; Chen et al., 2007a, 2007b).

However, the amphibolite-facies retrogression cannot be responsible for the large variations in composition of the UHP metamorphic rocks because there is no systematic correlation between the degrees of retrogression and the contents of water-soluble elements such as LILE and LREE (Tables 1 and 2). Both highly and slightly retrograde eclogites consistently show either enrichment or depletion of LILE and LREE (Table 1, Figs. 7 and 8). An investigation of mineral trace element distributions in UHP eclogites from the Dabie orogen demonstrated that the compositions of amphibolite-facies minerals are clearly controlled by the localized bulk composition of the microsite, with the composition of amphibole in particular depending on whether it replaced clinopyroxene or garnet (Sassi et al., 2000). A similar study reveals that the retrograde amphibole does not show enrichment of LILE as reflected by bulk-rock composition (Malaspina et al., 2006). These results indicate that the large variations of some elements in the UHP metamorphic rocks are unlikely caused by fluid-induced amphibolite-facies retrogression. Therefore, both the metamorphic dehydration during the continental subduction and the amphibolite-facies retrogression during the exhumation cannot significantly modify the element compositions of the UHP metamorphic rocks.

6.2. Melt-induced element mobility

Based on the several lines of evidence from experiments and natural rocks, Hermann et al. (2006) and Spandler et al. (2007) proposed that hydrous quartzo-feldspathic melt rather than aqueous fluid is the efficient medium to transfer significant amounts of trace elements from the slab to the mantle wedge. The melt-induced element mobility is also concordant with the geochemical variations in the UHP metamorphic rocks (Table 2). For the first core segment, eclogite I5A has the highest SiO_2 content (60.8%) but the lowest Ni (68.4 ppm) and Cr (94.1 ppm) contents, the other eclogites have relatively higher Ni contents of 80–129 ppm and Cr contents of 140–209 ppm. Similarly, amphibolite II8A from the second core segment has the highest SiO_2 content (57.5%) but the lowest Ni (24.4 ppm) and Cr (50 ppm) contents compared to the other eclogites and amphibolites that have relatively higher Ni contents of 37.6–74.7 ppm and Cr contents of 53.4–137 ppm. However, their Mg# numbers are similar to each other from the same core segment. In this regard, depletion of Ni and Cr in these samples would be caused by metasomatism of hydrous granitic melt rather than aqueous fluid.

Granitic melt formed by partial melting of the felsic gneiss at high pressures are characterized by low FeO, MgO, CaO, Cr and Ni contents but high SiO_2, total alkali ($Na_2O + K_2O$), LILE and LREE contents (Patiño Douce and McCarthy, 1998; Hermann and Green, 2001; Patiño Douce, 2005; Wallis et al., 2005). Metasomatism of the eclogites by such a melt would result in increases in SiO_2, alkali, LILE and LREE contents but decreases in FeO, MgO, CaO, Cr and Ni contents. However, their Mg# numbers will not change significantly because of the low FeO and MgO contents of granitic melt. These features are well consistent with those for some CCSD-MH samples of eclogite and amphibolite (I5A, I7A, II1A, II1(2)A and II8A), which have high SiO_2, alkali, LILE and LREE contents, but low FeO, MgO, CaO, Cr and Ni contents and Mg# numbers comparable to the other eclogites and amphibolites from the same core segment (Table 2 and Fig. 4). In addition, these samples have relatively high HFSE (i.e., Nb, Ta, Zr and Hf) contents (Table 2 and Fig. 8a and c). It is commonly accepted that the HFSE are water-insoluble elements and thus their content elevation is also related to melt—rather than fluid-induced metasomatism. This also accounts for the distinct correlations between SiO_2 and HFSE such as Zr (Fig. 4). On the other hand, the strong depletion of LREE and LILE in some eclogites (I13A and I14A, Fig. 7a and Fig. 8a) may result from extraction of partial melts with LREE and LILE enrichment. In fact, phengite is absent in these samples, possibly suggesting partial melting by breakdown of hydrous minerals during the exhumation of the deeply subducted continental crust.

The melt-induced element mobility may be responsible for the observed variations in composition of the CCSD-MH UHP metamorphic rocks at the contact of different lithologies. While the amphibolite–eclogite transition does not show considerable changes in SiO_2, LILE and LREE concentrations (Fig. 6), the changes are significant for retrograde eclogite I5A and amphibolite II8A at the transition to gneiss (Figs. 5 and 6). Eclogite I5A and amphibolite II8A have andesitic compositions with high contents of SiO_2 (57.5 to 60.8%), Rb (52.9–65.1 ppm) and K_2O (~2.6%) (Table 2). Their protoliths were originally of basaltic compositions as inferred from Mg# number comparable to the other eclogites and amphibolies from the same core segment. As argued above, metasomatism for eclogite I5A and amphibolite II8A would occur in the initial stage of exhumation because both prograde dehydration and amphibolite-facies retrogression cannot cause such composition variations. Because of the difference in the compositions and mineral assemblages between eclogite and gneiss, the consistent increases in SiO_2, K_2O, Rb, Ba and LREE concentrations for the two samples of metabasite were clearly caused by mass transfer via melt migration from the gneiss to eclogite or amphibolite.

In response to this mass transfer, a decrease in SiO_2 but consistent increases in Ba and LREE also occur in gneisses I4A and I3A at the transition to the eclogite (Fig. 5). In addition, increases in Rb and LREE in eclogites II1(2)A and II1A are also associated with the changes in SiO_2 and K_2O (Fig. 6). Petrographically, amphibolite-facies overprinting is significant for these samples of both eclogite and granitic gneiss (Fig. 3). Thus the lithological contrasts and fractures are favorite places for the mass transfer by melt migration, and for amphibolite-facies retrogression by fluid infiltration.

As illustrated in Figs. 5 and 6, there are no regular variations in contents of LREE and LILE (i.e., Rb, Ba and K) with sample localities, except the few samples at the transition between eclogite and gneiss. If the loss and gain of these elements in the eclogite and amphibolite can be ascribed to melt extraction and incorporation in the initial stage of exhumation, it would at most be a local behavior in a limited open-system at the lithological contrasts and fractures. Similarly, there are no regular variations in the degrees of amphibolite-facies retrogression with the sample localities. Therefore, retrograde fluid flow was not pervasive but localized and channelized. This suggestion is also supported by the study of stable isotopes in the Dabie–Sulu UHP rocks, which shows the O isotope heterogeneity that were preserved not only on outcrop scales but also on hand-specimen scales (Rumble et al., 2003; Zheng et al., 2003). A profile study of mineral O isotopes in CCSD-MH core samples shows O isotope heterogeneities between the different and same lithologies on scales of about 20–50 cm, corresponding to the maximum scales of fluid mobility during the continental collision (Chen et al., 2007b). Because the hydrous melt also contains the substantial amounts of aqueous fluid, it is capable of transporting both water-soluble and -insoluble elements during the subduction-zone metamorphism.

The granitic gneiss from the same CCSD-MH core segment has relatively homogeneous major and trace element compositions compared with the eclogite and amphibolite (Table 2 and Fig. 4). It has the typical features of continental crust, showing consistently enrichment of LREE and LILE but negative anomalies of HFSE (i.e., Nb, Ta and Ti) and P (Fig. 7b and d, Fig. 8b and d). However, some of the gneisses show negative Pb anomalies (Fig. 8c and d), which is not expected for the continental granitic rocks and for fluid-induced metasomatism. Wallis et al. (2005) obtained zircon U–Pb ages of 230 to 200 Ma for deformed K-feldspar-rich dikes in the Sulu orogen. Consistency of the dike emplacement with the tremendous Triassic ages for the Dabie–Sulu UHP metamorphism is another indication of the presence of melt during the continental collision. Because the granitic dikes formed by melting of felsic gneiss during the exhumation in the Sulu orogen have relatively high Pb contents of 26–38 ppm (Wallis et al., 2005), the extraction of such a melt would result in a decrease of Pb content in the residual gneiss. This is possibly responsible for the observed negative Pb anomalies in the gneisses.

6.3. Partial melting during exhumation

There are increasing lines of evidence that partial melting occurred in UHP gneissic rocks during slab exhumation (Auzanneau et al., 2006; Hermann et al., 2006; and references therein). For UHP metamorphic rocks in the Kokchetav Massif, it was suggested from lithochemical variations that diamond-bearing gneisses are melt-depleted rocks formed by significant melt extraction (Shatsky et al., 1995, 1999; Dobrestov and Shatsky, 2004). A detailed study of zircon from the diamond-bearing gneisses inferred that most of the zircon grains formed in the presence of hydrous granitic melt (Hermann et al., 2001). It has been suggested that partial melting of UHP gneisses in the Western Gneiss Complex and the Dabie–Sulu orogenic belt also occurred during exhumation (Auzanneau et al., 2006; Hermann et al., 2006). Findings of polyphase silicate inclusions within garnet and/or clinopyroxene in the Kokchetav Massif and the Erzgebirge of Germany (Hwang et al., 2001; Stökhert et al., 2001; Korsakov and Hermann, 2006) provide the most compelling evidence for the presence of hydrous granitic melts because both mineral assemblages and compositions of the these inclusions are very similar to felsic melts.

The occurrence of granitic melts in the CCSD-MH UHP metamorphic rocks is supported by the following petrographic observations: (1) occurrence of biotite + plagioclase coronas around phengite in some samples of eclogite and gneiss (Fig. 3c and f), indicating melt generation by phengite breakdown (Auzanneau et al., 2006); (2) aggregate of granitic minerals such as quartz, feldspar and biotite in some gneisses (Fig. 3f), suggesting the presence of hydrous granitic melt (Hermann et al., 2006); (3) occurrence of felsic vein in some eclogites and gneisses (Fig. 3b and Table 1), which may represent melt channelway. The local accumulation of felsic minerals suggests microscale transport of granitic melts relative to the host rocks. The distance that such melts can transport before crystallization depends on the topology of the melt reactions and the degree of melt segregation from the restite (Clemens and Droop, 1998). Fluid-saturated melts generated by muscovite dehydration reactions are unlikely to ascend far before crystallization (Harris et al., 1995). Thus, the partial melts did not escape from the host gneiss, resulting in a kind of metatexite migmatites (Sawyer, 1999).

Because a pervasive flow of aqueous fluid is unlikely to occur at depths beyond the uppermost few kilometers of crust (Yardley and Valley, 1997), fluid-absent melting by breakdown of hydrous minerals is a possible mechanism for granitic melt generation during exhumation (Auzanneau et al., 2006; Hermann et al., 2006). In the case of fluid-absent melting at given P–T conditions, the possibility of dehydration melting in the continental crust will mainly depend on the following factors (Clemens, 2006): (1) the available H_2O content of rock (as expressed by the hydrous mineral content); (2) the thermal stability of the hydrous mineral assemblage (the proportion of hydrous minerals that break down during melting); (3) the abundance of other phases required for the melting reactions to take place (e.g., quartz and feldspars). In other words, the quantity, dynamic properties, and chemical composition of these partial melts depend on the chemistry of protolith, the nature of melting reaction, the presence or absence of a fluid phase (and its composition), and pressure and temperature.

Phengite is the principal hydrous phase in UHP metamorphic rocks, its stability during prograde and retrograde UHP metamorphism of continental crust is very important to the partial melting in felsic UHP rocks (Hermann et al., 2006). If peak UHP metamorphic conditions are at relatively low temperatures and cooling occurs during the initial exhumation, as in the case of the Dora Maria Massif, phengite is stable during the bulk evolution of prograde and retrograde metamorphism and the UHP assemblages are well preserved (Chopin et al., 1991; Hermann, 2003). In contrast, if peak UHP metamorphic temperatures are greater than 750 °C and decompression is nearly isothermal or occurs with an increase in temperature, fluid-absent melting of phengite occurs during the exhumation of felsic UHP rocks (Hermann et al., 2006). This is well documented in examples like the Sulu orogen in China (Nakamura and Hirajima, 2000) and Ulten zone in the Italian Alps (Tumiati et al., 2003).

The *P–T* conditions of 750–850 °C and 2.8–4.5 GPa have been obtained for the UHP eclogite-facies regime in the Sulu orogen (e.g., Liou et al., 1998; Nakamura and Hirajima, 2000; Yao et al., 2000; Zhang et al., 2000; Liu et al., 2004c; Xu et al., 2006). The similar results are also obtained for the eclogites from CCSD-MH (Zhang et al., 2006a). Granulite-facies metamorphism, which postdates the peak UHP eclogite-facies metamorphism but predates the amphibolite-facies overprinting, has been reported in this region (e.g., Wang et al., 1993; Nakamura and Hirajima, 2000; Yao et al., 2000). Thus, an increase in temperature at decreasing pressure would occur at the initial exhumation of the deeply subducted continental crust. An in-situ study of trace elements in minerals from CCSD-MH eclogite also suggests short-lived heating during the exhumation (Zong et al., 2007). Therefore, the "hot" exhumation is evident for the UHP metamorphic rocks in the Sulu orogen. This process may be responsible for resetting of garnet Lu-Hf chronometric systems that resulted in consistent isochron ages of 219.6 to 223.4 Ma for garnet-omphacite minerals from UHP eclogites in the Dabie-Sulu orogenic belt (Schmidt et al., 2007).

Fig. 10 delineate the *P–T* path representative of the UHP lithological units in the Sulu orogen, in combination with experimental data available for phengite stability in intermediate to felsic rocks (Table 5). It appears that the "hot" exhumation is capable of causing the partial melting of UHP metamorphic rocks by phengite breakdown at about 830 °C and 3.8 GPa during the initial stage of exhumation (point A). On the other hand, phengite decomposition could also occur at a relatively wide *P–T* range from 850 to 750 °C at 2.3 to 1.1 GPa (from point B to C). While flush melting could occur in the diamond/coesite stability due to the heating at decreasing pressure in the first stage of exhumation, protracted melting would be significant at the maximum temperature and afterwards at the HP eclogite-facies conditions in the second stage of exhumation. In either case, the partial melting during the "hot" exhumation can account for the element mobility at the transitions between the different lithologies in the CCSD-MH core samples. As presented above, both petrographic observations and geochemical analyses provide evidence for the occurrence of granitic melt during the "hot" exhumation.

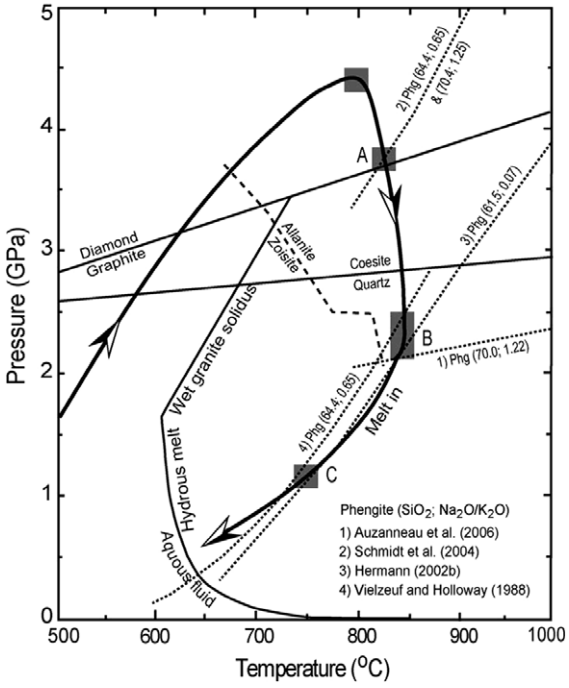

Fig. 10. Partial melting of intermediate to felsic rocks during the "hot" exhumation of deeply subducted continental crust. *P–T* path for UHP metamorphic rocks in the Sulu orogen is constructed after *P–T* estimates of Liou et al. (1998), Liu et al. (2004c) and Zhang et al. (2006a). Experimental data for phengite stability in intermediate to felsic rocks refers to Table 5. Dehydration melting due to phengite decomposition could take place at high *P–T* conditions (point A) and low *P–T* conditions (from point B to C), respectively, following the experimental data of Schmidt et al. (2004) for greywacke, Auzanneau et al. (2006) for metagraywack, Vielzeuf and Holloway (1988) for pelitic rock, and Hermann (2002b) for the KCMASH system. Zoisite and allanite stability fields are after the experimental results in the KCMASH system following Hermann (2002b). Wet solidus for the system granite + H_2O is after Huang and Wyllie (1981) and Holtz et al. (2001). Numbers in bracket after Phg denote the SiO_2 content and Na_2O/K_2O ratio of experimental rock system.

7. CONSTRAINTS ON PROTOLITH ORIGIN

7.1. Eclogite

The element and isotope compositions of high-grade metamorphic rocks have generally been used to deduce their protolith nature and tectonic setting (e.g., Culshaw and Dostal, 1997; Munyanyiwa et al., 1997; Jahn, 1998; Jahn et al., 2003, 2005; John et al., 2003; Volkova et al., 2004). One of the important prerequisites is that the protolith compositions reflected by these element and isotope systems have not suffered significant modification. While LILE and LREE may be modified by subduction-zone metamorphism, HFSE and HREE can be used to identify the protolith origin.

Although the eclogite and amphibolites from CCSD-MH show large scatters in LILE and LREE, HFSE and HREE contents do not show significant variations in the most eclogites (Figs. 7a, c and 8a and c). This indicates that HFSE and HREE are of relative immobility during the

Table 5
Experimental data for phengite stability field in intermediate-felsic rocks

Lithology	SiO_2	Na_2O	K_2O	H_2O	Na_2O/K_2O	P (GPa)	T (°C)	Reference
Metagreywacke	69.99	2.95	2.41	1.43	1.22	0.5–5.0	800–950	Auzanneau et al. (2006)
Greywacke	70.4	3	2.4	1.5	1.25	3.5–7.5	740–1180	Schmidt et al. (2004)
Pelite	64.4	1.7	2.6	2.1	0.65	3.5–7.5	740–1180	Schmidt et al. (2004)
P1 (diorite)	61.5	0.2	3	0	0.07	2.0–4.5	680–1050	Hermann (2002b)
Pelitic rock	64.35	1.66	2.56	2.15	0.65	0.2–2	600–1250	Vielzeuf and Holloway (1988)

continental subduction-zone metamorphism and thus can be used to deduce the protolith nature of eclogites. Most Dabie–Sulu eclogites from outcrops and from CCSD cores have high Ti/V ratios (>20), Zr/Y ratios (>3) and Y/Nb ratios (>4) (Jahn, 1998; Jahn et al., 2003; Zhang et al., 2006a). This suggests that their protoliths have geochemical affinity to the continental basalt rather than to the island-arc tholeiite (Pearce and Norry, 1979; Shervais, 1982).

There are significant differences in some major and trace element compositions of eclogite and granitic gneiss between the two core segments (Figs. 4, 7 and 8), implying different origins of protolith between them. Although LREE in some eclogites have been modified by the subduction-zone metamorphism, the difference in $\varepsilon_{Nd}(t)$ values at $t = 220$ Ma is significant for them. As shown in Fig. 11, the eclogites from the two core segments have the contrasting features in whole-rock Nd and garnet O isotope compositions. Those from the second core segment have lower $\varepsilon_{Nd}(t)$ values than the first core segment, but resemble most Dabie–Sulu outcrop eclogites (Jahn, 1998; Li et al., 2000; Chen et al., 2002; Jahn et al., 2003; Tang et al., 2007b). This suggests that the CCSD-MH eclogites have their protoliths from contrasting sources, with more components of juvenile crust in the first core segment than in the second core segment.

7.2. Granitic gneiss

The granitic gneisses from the two core segments have significantly different bulk chemical compositions (Fig. 4), but they all show enrichments in the water-soluble elements (except Pb) but depletion in the water-insoluble elements (Fig. 8b and d). Thus their protolith has the geochemical nature of evolved continental crust (e.g., Huang et al., 2006; Wu et al., 2006b). Like the eclogites, they also exhibit the contrasting features in whole-rock Nd and garnet O isotope compositions (Fig. 11). The gneisses from the second core segment also have lower $\varepsilon_{Nd}(t)$ values and old model Nd ages than the first core segment (Table 4), but resembles the large-scale granitic gneiss outcropped along the Dabie–Sulu orogenic belt (Li et al., 2000; Ma et al., 2000; Chen et al., 2002; Tang et al., 2007b). This suggests that the CCSD-MH gneisses also have their protoliths from contrasting sources, with more components of juvenile crust in the first core segment than in the second core segment.

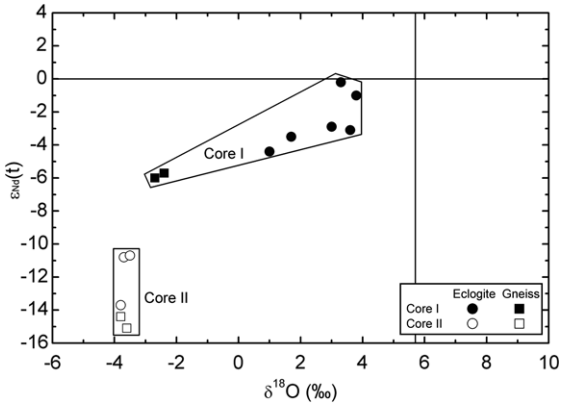

Fig. 11. Relationship between whole-rock Nd and garnet O isotope compositions for eclogite and gneiss from CCSD-MH. The initial Nd isotope ratios are calculated at $t = 220$ Ma. The vertical line denotes the $\delta^{18}O$ values for the normal mantle. Garnet $\delta^{18}O$ values are from Zhao et al. (2007).

The granitic gneiss from the first core segment has the relatively high $\varepsilon_{Nd}(t)$ values and young model Nd ages close to those of the eclogite, indicating that their protoliths are the same type of bimodal igneous rocks that probably result from reworking of juvenile crust (Zheng et al., 2006, 2007). On the other hand, the gneiss and eclogite from the second core segment have the relatively low $\varepsilon_{Nd}(t)$ values and old model Nd ages that are consistent with those of the granitic gneiss and eclogite now widely outcropped along the Dabie–Sulu orogenic belt. This suggests that their protoliths are also the other same type of bimodal igneous rocks that are possibly derived from partial melting of ancient continental lithosphere. Both eclogite and gneiss from the first core segment are respectively enriched in Mg but depleted in Fe relative to those from the second core segment (Fig. 4), suggesting a significant difference in their protolith origin. In this context, dual-bimodal compositions are recorded in the CCSD-MH samples.

Bimodal igneous rocks of mid-Neoproterozoic ages from the South China Block have been studied intensively with respect to their genetic relationship to breakup of the supercontinent Rodinia (Li et al., 2003a,b; Zheng et al., 2004, 2006, 2007; Huang et al., 2006; Wu et al., 2006b; Tang et al., 2007b). They can be grouped into two periods, with pre-rift magmatism at 800 to 830 Ma and syn-rift magmatism at 780 to 740 Ma (Li et al., 2003b; Zheng et al., 2004, 2006; Wu et al., 2006b; Tang et al., 2007b). Previous studies of zircon U–Pb geochronology and geochemistry have demonstrated that the protoliths of Dabie–Sulu UHP eclogite and granitic gneiss are the mid-Neoproterozoic bimodal igneous rock that formed in rift tectonic zones along the northern margin of the South China Block (Ames et al., 1996; Hacker et al., 1998; Zheng et al., 2004, 2006; Huang et al., 2006; Tang et al., 2007b). The present study has identified the two types of bimodal magmatism with contrasting origins for the protoliths of

eclogite and granitic gneiss from the CCSD-MH cores in the Sulu orogen. The contemporaneous occurrence of dual bimodal igneous rocks is clearly be a manifestation of the high heat flow and lithosphere-scale faults that are associated with tectonic advance from supercontinental rift to breakup, with volcanic rift margins as the best site for growth and reworking of juvenile crust (Zheng et al., 2006, 2007).

8. CONCLUSIONS

Significant mobility of elements did exist during continental subduction-zone metamorphism, particularly for such water-soluble elements as LILE and LREE. UHP eclogites from two CCSD-MH core segments in the Sulu orogen show large variations in major and some trace elements such as LILE (e.g., Rb, Ba and K) and LREE, but relatively limited ranges in such water-insoluble elements as HFSE and HREE. Some eclogites have andesitic compositions with high SiO_2, LREE and LILE contents, which likely result from metasomatism of granitic melt formed by partial melting of the associated felsic UHP gneisses during exhumation of deeply subducted continental crust. Significant LREE and LILE depletion occurs in some eclogites, possibly due to melt extraction. In particular, significant variations of SiO_2, LREE and LILE contents occur at the contact between different lithologies in concordance with petrographic changes, implying the occurrence of hydrous melt and its associated element mobility between different slab components during the exhumation. Therefore, partial melting of continental crust took place locally during the ''hot'' exhumation, resulting in significant mass transfer within the UHP slabs. Nevertheless, the efficient transport of elements only occurs on small scales and is thus limited in local open-systems at the lithological contrasts and fractures.

By eliminating the metamorphic modification during the continental subduction-zone metamorphism, two types of bimodal magmatism with contrasting origins can be deduced for protoliths of UHP eclogite and granitic gneiss from the CCSD-MH cores. The first type of bimodal igneous rocks has relatively high $\varepsilon_{Nd}(t)$ values and young model Nd ages, indicating that their origin from reworking of juvenile crust. The second type of bimodal igneous rocks show relatively low $\varepsilon_{Nd}(t)$ values and old model Nd ages, suggesting that their derivation from partial melting of ancient continental lithosphere. In either case, the dual bimodal protoliths of UHP metaigneous rocks were emplaced in a rift tectonic zone during the middle Neoproterozoic, with overprinting of high-T meteoric-hydrothermal alteration.

ACKNOWLEDGMENTS

This study was supported by funds from the Chinese Ministry of Science and Technology (2003CB716501), the Natural Science Foundation of China (40673009) and the Program for New Century Excellent Talents in University (NCET-05-0552). Thanks are due to Drs. Yaoling Niu and J.G. Liou for their comments on early versions of the manuscript. We are grateful to Drs. J. Hermann and T. Zack for their constructive comments, to Dr. A. Brandon for his editorial handling of the manuscript.

REFERENCES

Ames L., Zhou G. Z. and Xiong B. C. (1996) Geochronology and isotopic character of ultrahigh-pressure metamorphism with implications for collision of the Sino-Korean and Yangtze cratons, central China. *Tectonics* **15**, 472–489.

Arculus R. J., Lapierre H. and Jaillard E. (1999) Geochemical window into subduction and accretion processes: Raspas metamorphic complexm Ecuador. *Geology* **27**, 547–550.

Auzanneau E., Vielzeuf D. and Schmidt M. W. (2006) Experimental evidence of decompression melting during exhumation of subducted continental crust. *Contrib. Mineral. Petrol.* **152**, 125–148.

Becker H., Jochum K. P. and Carlson R. W. (2000) Trace element fractionation during dehydration of eclogites from high-pressure terranes and the implications for element fluxes in subduction zones. *Chem. Geol.* **163**, 65–99.

Breeding C. M., Ague J. J. and Bröcker M. (2004) Fluid-metasedimentary rock interactions in subduction-zone mélange: implications for the chemical composition of arc magmas. *Geology* **32**, 1041–1044.

Carswell D. A. and Compagnoni R. (2003) Introduction with review of the definition, distribution and geotectonic significance of ultrahigh pressure metamorphism. *EMU Notes Mineral.* **5**, 3–9.

Chalot-Prat F., Ganne J. and Lombard A. (2003) No significant element transfer from the oceanic plate to the mantle wedge during subduction and exhumation of the Tethys lithosphere (Western Alps). *Lithos* **69**, 69–103.

Chen B., Jahn B.-M., Ye K. and Liu J. B. (2002) Cogenetic relationship of the Yangkou gabbro-to-granite unit, Su–Lu terrane, eastern China, and implications for UHP metamorphism. *J. Geol. Soc. Lond.* **159**, 457–467.

Chen R.-X., Zheng Y.-F., Gong B., Zhao Z.-F., Gao T-. S., Chen B. and Wu Y.-B. (2007a) Origin of retrograde fluid in ultrahigh-pressure metamorphic rocks: constraints from mineral hydrogen isotope and water content changes in eclogite-gneiss transitions in the Sulu orogen. *Geochim. Cosmochim. Acta* **71**, 2299–2325.

Chen R.-X., Zheng Y.-F., Gong B., Zhao Z.-F., Gao T.-S., Chen B. and Wu Y.-B. (2007b) Oxygen isotope geochemistry of ultrahigh-pressure metamorphic rocks from 200–4000 m core samples of the Chinese Continental Scientific Drilling. *Chem. Geol.* **242**, 51–75.

Chopin C. (1984) Coesite and pure pyrope in high-grade blueschists of the western Alps: a first record and some consequences. *Contrib. Mineral. Petrol.* **86**, 107–118.

Chopin C., Henry C. and Michard A. (1991) Geology and petrology of the coesite-bearing terrain, Dora-Maira Massif, Western Alps. *Eur. J. Mineral.* **3**, 263–291.

Clemens J. D. (2006) Melting of the continental crust: fluid regimes, melting reactions, and source-rock fertility. In *Evolution and Differentiation of the Continental Crust* (eds. M. Brown and T. Rushmer). Cambridge University Press, Cambridge, pp. 296–327.

Clemens J. D. and Droop G. R. T. (1998) Fluids, P–T paths and the fate of anatectic melts in the Earth's crust. *Lithos* **44**, 21–36.

Cong B. L. (1996) *Ultrahigh-Pressure Metamorphic Rocks in the Dabieshan–Sulu Region of China*. Science Press, Beijing, 224 pp.

Culshaw N. and Dostal J. (1997) Sand Bay gneiss association, Grenville Province, Ontario: a Grenvillian rift- (and -drift) assemblage stranded in the Central Gneiss Belt? *Precambr. Res.* **85**, 97–113.

dePaolo D. J. (1988) *Neodymium Isotope Geochemistry: An Introduction*. Springer-Verlag, New York, 181 pp.

Dobrestov N. L. and Shatsky V. S. (2004) Exhumation of high-pressure rocks of the Kokchetav massif: facts and models. *Lithos* **78**, 307–318.

Ernst W. G. and Liou J. G. (1999) Overview of UHP metamorphism and tectonics in well-studied collisional orogens. *Int. Geol. Rev.* **41**, 477–493.

Ferrando S., Frezzotti M. L., Dallai L. and Compagnoni R. (2005) Multiphase solid inclusions in UHP rocks (Su-Lu, China): remnants of supercritical silicate-rich aqueous fluids release during continental subduction. *Chem. Geol.* **223**, 68–81.

Fu B., Touret J. L. R. and Zheng Y. F. (2001) Fluid inclusions in coesite-bearing eclogites and jadeite quartzite at Shuanghe, Dabie Shan (China). *J. Metamorph. Geol.* **19**, 529–545.

Hacker B. R., Ratschbacher L., Webb L. E., Ireland T. R., Walker D. and Dong S. (1998) U/Pb zircon ages constrain the architecture of the ultrahigh-pressure Qinling–Dabie orogen, China. *Earth Planet. Sci. Lett.* **161**, 215–230.

Harris N., Ayres M. and Massey J. (1995) Geochemistry of granitic melts produced during the incongruent melting of muscovite—implications for the extraction of Himalayan leucogranite magmas. *J. Geophys. Res.* **B100**, 15767–15777.

Hawkesworth C. J., Hergt J. M., Ellam R. M. and McDermott F. (1991) Element fluxes associated with subduction related magmatism. *Philos. Trans. Roy. Soc.* **A335**, 393–405.

Hermann J. (2002a) Allanite: Thorium and light rare earth element carrier in subducted crust. *Chem. Geol.* **192**, 289–306.

Hermann J. (2002b) Experimental constraints on phase relations in subducted continental crust. *Contrib. Mineral. Petrol.* **143**, 219–235.

Hermann J. (2003) Experimental evidence for diamond-facies metamorphism in the Dora-Maira massif. *Lithos* **70**, 163–182.

Hermann J. and Green D. H. (2001) Experimental constraints on high pressure melting in subducted crust. *Earth Planet. Sci. Lett.* **188**, 149–168.

Hermann J., Rubatto D., Korsakov A. and Shatsky V. S. (2001) Multiple zircon growth during fast exhumation of diamondiferous, deeply subducted continental crust (Kokchetav Massif, Kazakhstan). *Contrib. Mineral. Petrol.* **141**, 66–82.

Hermann J., Spandler C., Hack A. and Korsakov A. V. (2006) Aqueous fluids and hydrous melts in high-pressure and ultra-high pressure rocks: implications for element transfer in subduction zones. *Lithos* **92**, 399–417.

Holtz F., Becker A., Freise M. and Johannes W. (2001) The water-undersaturated and dry Qz–Ab–Or system revisited. Experimental results at very low water activities and geological implications. *Contrib. Mineral. Petrol.* **141**, 347–357.

Huang W. L. and Wyllie P. J. (1981) Phase relationships of S-type granite with H_2O to 35 kbar: muscovite granite from Harney Peak, south Dakota. *J. Geophys. Res.* **86**, 10515–10529.

Huang J., Zheng Y.-F., Zhao Z.-F., Wu Y.-B., Zhou J.-B. and Liu X. M. (2006) Melting of subducted continent: element and isotopic evidence for a genetic relationship between Neoproterozoic and Mesozoic granitoids in the Sulu orogen. *Chem. Geol.* **229**, 227–256.

Hwang S.-L., Shen P., Chu H.-T., Yui T.-F. and Lin C.-C. (2001) Gneiss of microdiamonds from melt and associated multiphase inclusions in garnet of ultrahigh-pressure gneiss from Erzgebirge, Germany. *Earth Planet. Sci. Lett.* **188**, 9–15.

Jahn B.-M. (1998) Geochemical and isotopic characteristics of UHP eclogites and ultramafic rocks of the Dabie orogen. In *When Continents Collide: Geochemistry of Ultrahigh-pressure Rocks* (eds. B. R. Hacker and J. G. Liou). Kluwer Academic Publishing, Dordrecht, pp. 203–239.

Jahn B.-M. and Condie K. C. (1995) Evolution of the Kaapvaal Craton as viewed from geochemical and Sm–Nd isotopic analyses of intracratonic pelites. *Geochim. Cosmochim. Acta* **59**, 2239–2258.

Jahn B.-M., Cornichet J., Cong B. L. and Yui T. F. (1996) Ultrahigh ε_{Nd} eclogites from an UHP metamorphic terrane of China. *Chem. Geol.* **127**, 61–79.

Jahn B.-M., Rumble D. and Liou J. G. (2003) Geochemistry and isotope tracer study of UHP metamorphic rocks. *EMU Notes Mineral.* **5**, 365–414.

Jahn B.-M., Liu X. C., Yui T.-F., Morin N. and Coz M. B.-L. (2005) High-pressure/ultrahigh-pressure eclogites from the Hong'an Block, East-Central China: geochemical characterization, isotope disequilibrium and geochronological controversy. *Contrib. Mineral. Petrol.* **149**, 499–526.

John T., Schenk V., Haase K., Scherer E. and Tembo F. (2003) Evidence for a Neoproterozoic ocean in south-central Africa from mid-oceanic-ridge-type geochemical signatures and pressure–temperature estimates of Zambian eclogites. *Geology* **31**, 243–246.

John T., Scherer E. E., Haase K. and Schenk V. (2004) Trace element fractionation during fluid-induced eclogititation in a subducting slab: trace element and Lu–Hf–Sm–Nd isotope systematics. *Earth Planet. Sci. Lett.* **227**, 441–456.

Kessel R., Ulmer P., Pettke T., Schmidt M. W. and Thompson A. B. (2005a) The water–basalt system at 4 to 6 GPa: Phase relations and second critical endpoint in a K-free eclogite at 700 to 1400 °C. *Earth Planet. Sci. Lett.* **237**, 873–892.

Kessel R., Schmidt M. W., Ulmer P. and Pettke T. (2005b) Trace element signature of subduction-zone fluids, melts and supercritical liquids at 120–180 km depth. *Nature* **437**, 724–727.

Kogiso T., Tatsumi Y. and Nakano S. (1997) Trace element transport during dehydration processed in the subduction oceanic crust: 1. Experiments and implications for the origin of ocean island basalts. *Earth Planet. Sci. Lett.* **148**, 193–205.

Korsakov A. V. and Hermann J. (2006) Silicate and carbonate melt inclusions associated with diamonds in deeply subducted carbonate rocks. *Earth Planet. Sci. Lett.* **241**, 104–118.

Kretz R. (1983) Symbols for rock-forming minerals. *Am. Mineral.* **68**, 277–279.

Liang X. R., Wei G. J., Li X. H. and Liu Y. (2003) Precise measured of $^{143}Nd/^{144}Nd$ and Sm/Nd ratios using multiple-collectors inductively coupled plasma-mass spectrometer (MC-ICPMS). *Geochimica* **32**, 91–96, in Chinese with English abstract.

Li S. G., Jagoutz E., Lo C.-H., Chen Y., Li Q. and Xiao Y. (1999) Sm/Nd, Rb/Sr, and $^{40}Ar/^{39}Ar$ isotopic systematics of the ultrahigh-pressure metamorphic rocks in the Dabie–Sulu Belt, central China: a retrospective view. *Int. Geol. Rev.* **41**, 1114–1124.

Li S.-G., Jagoutz E., Chen Y.-Z. and Li Q.-L. (2000) Sm–Nd and Rb–Sr isotopic chronology and cooling history of ultrahigh pressure metamorphic rocks and their country rocks at Shuanghe in the Dabie Mountains, Central China. *Geochim. Cosmochim. Acta* **64**, 1077–1093.

Li Y.-L., Zheng Y.-F., Fu B., Zhou J.-B. and Wei C.-S. (2001) Oxygen isotope composition of quartz-vein in ultrahigh-pressure eclogite from Dabieshan and implications for transport of high-pressure metamorphic fluid. *Phys. Chem. Earth (A)* **26**, 695–704.

Li X.-H., Liu Y., Tu X.-L., Hu G.-Q. and Zeng W. (2002) Precise determination of chemical compositions in silicate rocks using ICP-AES and ICP-MS: a comparative study of sample digestion techniques of alkali fusion and acid dissolution. *Geochimica* **31**, 289–294, in Chinese with English abstract.

Li X. H., Li Z. X., Ge W., Li W. X., Liu Y. and Wingate M. T. D. (2003a) Neoproterozoic granitoids in South China: crustal melting above a mantle plume at ca. 825 Ma? *Precambr. Res.* **122**, 45–83.

Li Z. X., Li X. H., Kinny P. D., Wang J., Zhang S. H. and Zhou H. (2003b) Geochronology of Neoproterozoic syn-rift magmatism in the Yangtze craton, South China and correlations with other continents: evidence for a mantle superplume that broke up Rodinia. *Precambr. Res.* **122**, 85–109.

Li X.-P., Zheng Y.-F., Wu Y.-B., Chen F. K., Gong B. and Li Y.-L. (2004) Low-*T* eclogite in the Dabie terrane of China: petrological and isotopic constraints on fluid activity and radiometric dating. *Contrib. Mineral. Petrol.* **148**, 443–470.

Liou J. G. (1999) Petrotectonic summary of less-intensively studied UHP regions. *Int. Geol. Rev.* **41**, 571–586.

Liou J. G., Zhang R. Y., Wang X., Eide E. A., Ernst W. G. and Maruyama S. (1996) Metamorphism and tectonics of high-pressure belts in the Dabie–Sulu region, China. In *The Tectonic Evolution of Asia* (eds. A. Yin and T. M. Harrison). Cambridge University Press, Cambridge, pp. 300–344.

Liou J. G., Zhang R. Y. and Ernst W. G. (1997) Lack of fluid during ultrahigh-*P* metamorphism in the Dabie–Sulu region, Eastern China. *Proc. Int. Geol. Congress* **17**(30), 141–155.

Liou J. G., Zhang R. Y., Ernst W. G., Rumble D. and Maruyama S. (1998) High-pressure minerals from deeply subducted metamorphic rocks. *Rev. Mineral.* **37**, 33–96.

Liu F. L. and Xu Z. Q. (2004) Fluid inclusions hidden in coesite-bearing zircons in ultrahigh-pressure metamorphic rocks from southwestern Sulu terrane in eastern China. *Chin. Sci. Bull.* **49**, 396–404.

Liu Y., Liu H.-C. and Li X.-H. (1996) Simultaneous and precise determination of 40 trace elements in rock samples using ICP-MS. *Geochimica* **25**, 552–558, in Chinese with English abstract.

Liu F. L., Xu Z. Q., Katayama I., Yang J. S., Maruyama S. and Liou J. G. (2001) Mineral inclusions in zircons of para- and orthogneiss from pre-pilot drillhole CCSD-PP1, Chinese Continental Scientific Drilling Project. *Lithos* **59**, 199–215.

Liu F. L., Xu Z. Q., Liou J. G., Katayama I., Masago H., Maruyama S. and Yang J. S. (2002) Ultrahigh-pressure mineral inclusions in zircons of gneissic core samples of the Chinese Continental Scientific Drilling Site in eastern China. *Eur. J. Mineral.* **14**, 499–512.

Liu F. L., Xu Z. Q., Liou J. G. and Song B. (2004a) SHRIMP U–Pb ages of ultrahigh-pressure and retrograde metamorphism of gneisses, south-western Sulu terrane, eastern China. *J. Metamorph. Geol.* **22**, 315–326.

Liu F. L., Xu Z. Q. and Xue H. M. (2004b) Tracing the protolith, UHP metamorphism, and exhumation ages of orthogneiss from the SW Sulu terrane (eastern China): SHRIMP U–Pb dating of mineral inclusion-bearing zircons. *Lithos* **78**, 411–429.

Liu F. L., Xu Z. Q. and Liou J. G. (2004c) Tracing the boundary between UHP and HP metamorphic belts in the southwestern Sulu terrane, eastern China: evidence from mineral inclusions in zircons from metamorphic rocks. *Int. Geol. Rev.* **46**, 409–425.

Liu F. L., Liou J. G. and Xu Z. Q. (2005) U–Pb SHRIMP ages recorded in the coesite-bearing zircon domains of paragneisses in the southwestern Sulu terrane, eastern China: new interpretation. *Am. Mineral.* **90**, 790–800.

Liu D. Y., Jian P., Kröner A. and Xu S. T. (2006) Dating of prograde metamorphic events deciphered from episodic zircon growth in rocks of the Dabie–Sulu UHP complex, China. *Earth Planet. Sci. Lett.* **250**, 650–666.

Liu Y.-H., Yang H.-J., Shau Y.-H., Meng F. C., Zhang J. X., Yang J. S., Xu Z. Q. and Yu S.-C. (2007) Compositions of high Fe–Ti eclogites from the Sulu UHP metamorphic terrane, China: HFSE decoupling and protolith characteristics. *Chem. Geol.* **239**, 64–82.

Ma C. Q., Ehlers C., Xu C. H., Li Z. C. and Yang K. G. (2000) The roots of the Dabieshan ultrahigh-pressure metamorphic terrane: constraints from geochemistry and Nd–Sr isotope systematics. *Precambr. Res.* **102**, 279–301.

Malaspina N., Hermann J., Scambelluri M. and Compagnoni R. (2006) Multistage metasomatism in ultrahigh-pressure mafic rocks from the North Dabie Complex (China). *Lithos* **90**, 19–42.

McDonough W. F. and Sun S.-S. (1995) The composition of the Earth. *Chem. Geol.* **120**, 223–253.

Munyanyiwa H., Hanson R. E., Blenkinsop T. G. and Treloar P. J. (1997) Geochemistry of amphibolites and quartzofeldspathic gneisses in the Pan-African Zambezi belt, northwest Zimbabwe: evidence for bimodal magmatism in a continental rift setting. *Precambr. Res.* **81**, 179–196.

Nakamura D. and Hirajima T. (2000) Granulite-facies overprinting of ultrahigh-pressure metamorphic rocks, northeastern Su-Lu region, eastern China. *J. Petrol.* **41**, 563–582.

Okay A. I., Xu S.-T. and Sengor A. M. C. (1989) Coesite form the Dabie Shan eclogites, central China. *Eur. J. Mineral.* **1**, 595–598.

Patiño Douce A. E. (2005) Vapor-absent melting of tonalite at 15–32 kbar. *J. Petrol.* **46**, 275–290.

Patiño Douce A. E. and McCarthy T. C. (1998) Melting of crustal rocks during continental collision and subduction. In *When Continents Collide* (eds. B. R. Hacker and J. G. Liou). Kluwer Academic, Correct, Netherlands, pp. 27–55.

Pearce J. A. and Norry M. J. (1979) Petrogenetic implications of Ti, Zr, Y, and Nb variations in volcanic rocks. *Contrib. Mineral. Petrol.* **25**, 956–983.

Polat A., Hofmann A. W. and Rosing M. T. (2002) Boninite-like volcanic rocks in the 3.7–3.8 Ga Isua greenstone belt, West Greenland: geochemical evidence for intra-oceanic subduction zone processes in the early Earth. *Chem. Geol.* **184**, 231–254.

Rumble D., Giorgis D., Oreland T., Zhang Z.-M., Xu H.-F., Yui T.-F., Yang J.-S., Xu Z.-Q. and Liou J. G. (2002) Low $\delta^{18}O$ zircons, U–Pb dating, and the age of the Qinglongshan oxygen and hydrogen isotope anomaly near Donghai in Jiangsu province, China. *Geochim. Cosmochim. Acta* **66**, 2299–2306.

Rumble D., Liou J. G. and Jahn B. M. (2003) Continental crust subduction and ultrahigh pressure metamorphism. *Treatise Geochem.* **3**, 293–319.

Rüpke L. H., Morgan J. P., Hort M. and Connolly J. A. D. (2002) Are the regional variations in Central American arc lavas due to differing basaltic versus peridotitic slab sources of fluids? *Geology* **30**, 1035–1038.

Sassi R., Harte B., Carswell D. A. and Han Y. J. (2000) Trace element distribution in Central Dabie eclogites. *Contrib. Mineral. Petrol.* **139**, 298–315.

Sawyer E. W. (1999) Criteria for the recognition of partial melting. *Phys. Chem. Earth (A)* **24**, 269–279.

Scambelluri M., Bottazzi P., Trommsdirff V., Vannucci R., Hermann J., Gomez-Pugnaire M. T. and Vizcaino V. L.-S. (2001) Incompatible element-rich fluids released by antigorite breakdown in deeply subducted mantle. *Earth Planet. Sci. Lett.* **192**, 457–470.

Schmidt M. W., Vielzeuf D. and Auzanneau E. (2004) Melting and dissolution of subducting crust at high pressures: the key role of white mica. *Earth Planet. Sci. Lett.* **228**, 65–84.

Schmidt A., Weyer S., Xiao Y., Hoefs J. and Brey G. P. (2007) Lu-Hf analysis of eclogites from the Dabie-Sulu terrains: constraints on the timing of eclogite-facies metamorphism. *Geochim. Cosmochim. Acta* **71**, A894.

Shatsky V. S., Sobolev N. V. and Vavilov M. A. (1995) Diamond-bearing metamorphic rocks of the Kokchetav Massif (northern Kazakhstan). In *Ultrahigh Pressure Metamorphism* (eds. R. G. Coleman and X. Wang). Cambridge University Press, Cambridge, UK, pp. 427–455.

Shatsky V. S., Jagoutz E., Sobolev N. V., Kozmenko O. A., Parkhomenko V. S. and Troesch M. (1999) Geochemistry and age of ultrahigh pressure metamorphic rocks from the Kokchetav massif (Northern Kazakhstan). *Contrib. Mineral. Petrol.* **137**, 185–205.

Sheng Y.-M., Xia Q.-K., Yang X.-Z. and Hao Y.-T. (2007) H_2O contents and D/H ratios of nominally anhydrous minerals from ultrahigh-pressure eclogites of the Dabie orogen, eastern China. *Geochim. Cosmochim. Acta* **71**, 2079–2103.

Shervais J. W. (1982) Ti–V plots and the petrogenesis of modern ophiolitic lavas. *Earth Planet. Sci. Lett.* **59**, 101–118.

Smith D. C. (1984) Coesite in clinopyroxene in the Caledonides and its implications for geodynamics. *Nature* **310**, 641–644.

Spandler C., Hermann J., Arculus R. and Mavrogenes J. (2003) Redistribution of trace elements during prograde metamorphism from lawsonite blueschist to eclogite facies: implications for deep subduction-zone processes. *Contrib. Mineral. Petrol.* **146**, 205–222.

Spandler C., Hermann J., Arculus R. and Mavrogenes J. (2004) Geochemical heterogeneity and element mobility in deeply subducted oceanic crust: insights from high-pressure mafic rocks from New Caledonia. *Chem. Geol.* **206**, 21–42.

Spandler C., Mavrogenes J. and Hermann J. (2007) Experimental constraints on element mobility from subducted sediments using high-*P* synthetic fluid/melt inclusions. *Chem. Geol.* **239**, 228–249.

Stalder R., Foley S. F., Brey G. P. and Horn I. (1998) Mineral aqueous fluid partitioning of trace elements at 900-1200 °C and 3.0–5.7 GPa: new experimental data for garnet, clinopyroxene, and rutile, and implications for mantle metasomatism. *Geochim. Cosmochim. Acta* **62**, 1781–1801.

Stökhert B., Duyster J., Trepman C. and Massonne H.-J. (2001) Microdiamond daughter crystals precipitated from supercritical COH + silicate fluids induced in garnet, Erzgebirge, Germany. *Geology* **29**, 391–394.

Tang H.-F., Liu C.-Q., Nakai S.-I. and Orihashi Y. (2007a) Geochemistry of eclogites from the Dabie–Sulu terrane, eastern China: new insights into protoliths and trace element behavior during UHP metamorphism. *Lithos* **95**, 441–457.

Tang J., Zheng Y. -F., Wu Y. -B., Gong B., Zha X. P. and Liu X. M. (2007b) Zircon U–Pb age and geochemical constraints on the tectonic affinity of the Jiaodong terrane in the Sulu orogen. *China. Precambr. Res*, doi:10.1016/j.precamres.2007.09.008.

Tatsumi Y. and Eggins S. (1995) *Subduction Zone Magmatism*. Blackwell Science, Oxford, 211 pp.

Tribuzio R., Messiga B., Vannucci R. and Bottazzi P. (1996) Rare earth element redistribution during high-pressure-low-temperature metamorphism in ophiolitic Fe-gabbros (Liguria, northwestern Italy); implications for light REE mobility in subduction zones. *Geology* **24**, 711–714.

Tumiati S., Thöni M., Nimis P., Martin S. and Mair V. (2003) Mantle–crust interactions during Variscan subduction in the Eastern Alps (Nonsberg-Ulten Zone): geochronology and new petrological constraints. *Earth Planet. Sci. Lett.* **210**, 509–526.

Vielzeuf D. and Holloway J. R. (1988) Experimental determination of the fluid-absent melting reactions in the pelitic system: consequences for crustal differentiation. *Contrib. Mineral. Petrol.* **98**, 257–276.

Volkova N. I., Frenkel A. E., Budanov V. I. and Lepezin G. G. (2004) Geochemical signatures for eclogite protolith from the Maksyutov Complex, South Urals. *J. Asian Earth Sci.* **23**, 745–759.

Wallis S., Tsuboi M., Suzuki K., Fanning M., Jiang L. and Tanaka T. (2005) Role of partial melting in the evolution of the Sulu (eastern China) ultrahigh-pressure terrane. *Geology* **33**, 129–132.

Wang X.-M., Liou J.-G. and Mao H.-K. (1989) Coesite-bearing eclogites from the Dabie Mountains in central China. *Geology* **17**, 1085–1088.

Wang Q. C., Ishiwatari A., Zhao Z., Hirajima T., Enami M., Zhai M., Li J. and Cong B. L. (1993) Coesite-bearing granulite retrograded from eclogite in Weihai, eastern China. *Eur. J. Mineral.* **5**, 141–152.

Wu Y.-B., Zheng Y.-F., Zhao Z.-F., Gong B., Liu X. M. and Wu F.-Y. (2006a) U–Pb, Hf and O isotope evidence for two episodes of fluid-assisted zircon growth in marble-hosted eclogites from the Dabie orogen. *Geochim. Cosmochim. Acta* **70**, 3743–3761.

Wu R.-X., Zheng Y.-F., Wu Y.-B., Zhao Z.-F., Zhang S.-B., Liu X. M. and Wu F.-Y. (2006b) Reworking of juvenile crust: element and isotope evidence from Neoproterozoic granodiorite in South China. *Precambr. Res.* **146**, 179–212.

Xia Q.-K., Sheng Y.-M., Yang X.-Z. and Yu H.-M. (2005) Heterogeneity of water in garnets from UHP eclogites, eastern Dabieshan, China. *Chem. Geol.* **224**, 237–246.

Xia Q.-K., Yang X.-Z., Deloule E., Sheng Y.-M. and Hao Y.-T. (2006) Water in the lower crustal granulite xenoliths from Nushan, SE China. *J. Geophys. Res.* **111**, B11202. doi:10.1029/2006JB 004296.

Xiao Y. L., Sun W. D., Hoefs J., Simon K., Zhang Z. M., Li S. G. and Hofmann A. W. (2006a) Making continental crust through slab melting: constraints from niobium–tantalum fractionation in UHP metamorphic rutile. *Geochim. Cosmochim. Acta* **70**, 4770–4782.

Xiao Y., Zhang Z.-M., Hoefs J. and van den Kerkhof A. (2006b) Ultrahigh-pressure metamorphic rocks from the Chinese Continental Scientific Drilling Project-II. Oxygen isotope and fluid inclusion distributions through vertical sections. *Contrib. Mineral. Petrol.* **152**, 443–458.

Xu Z.-Q. (2004) The scientific goals and investigation progresses of the Chinese Continental Scientific Drilling Project. *Acta Petrol. Sin.* **20**, 1–8, in Chinese with English abstract.

Xu S. T., Okay A. I., Ji S. Y., Sengor A. M. C., Su W., Liu Y. C. and Jiang L. L. (1992) Diamond from the Dabie Shan metamorphic rocks and its implication for tectonic setting. *Science* **256**, 80–82.

Xu Z. Q., Yang W. C., Zhang Z. M. and Yang T. N. (1998) Scientific significance and site-selection researches of the first Chinese continental scientific deep drillhole. *Continental Dyn.* **3**, 1–13.

Xu S. T., Liu Y. C., Chen G. B., Roberto C., Franco R., He M. C. and Liu H. F. (2003) New finding of microdiamonds in eclogites from Dabie–Sulu region in central-eastern China. *Chin. Sci. Bull.* **48**, 988–994.

Xu S. T., Liu Y. C., Chen G. B., Ji S. Y., Ni P. and Xiao W. S. (2005) Microdiamonds, their classification and tectonic implications for the host eclogites from the Dabie and Su–Lu regions in central eastern China. *Mineral. Mag.* **69**, 509–520.

Xu Z. -Q., Zeng L. -S., Liu F. -L., Yang J. -S., Zhang Z. -M., McWilliams M. and Liou J. G. (2006) Polyphase subduction and exhumation of the Sulu high-pressure-ultrahigh-pressure metamorphic terrane. In *Ultrahigh-Pressure Metamorphism: Deep Continental Subduction* (eds. B. R. Hacker, W. C. McClelland, and J. G. Liou). Geol. Soc. Am. Spec. Paper 403, pp. 93–113.

Yao Y. P., Ye K., Liu J. B., Cong B. L. and Wang Q. C. (2000) A transitional eclogite- to high pressure granulite-facies overprint on coesite–eclogite at Taohang in the Sulu ultrahigh-pressure terrane, Eastern China. *Lithos* **52**, 109–120.

Yardley B. W. D. and Valley J. W. (1997) The petrologic case for a dry lower crust. *J. Geophys. Res.* **102**, 12173–12185.

Zack T. and John T. (2007) An evaluation of reactive fluid flow and trace element mobility in subducting slabs. *Chem. Geol.* **237**, 199–216.

Zack T., Rivers T. and Foley S. F. (2001) Cs-Rb-Ba systematics in phengite and amphibole: an assessment of fluid mobility at 2.0 GPa in eclogites from Trescolmen, Central Alps. *Contrib. Mineral. Petrol.* **140**, 651–669.

Zack T., Foley S. F. and Rivers T. (2002) Equilibrium and disequilibrium trace element partitioning in hydrous eclogites (Trescolmen, Central Alps). *J. Petrol.* **43**, 1947–1974.

Zhang Z. M., Xu Z. Q. and Xu H. F. (2000) Petrology of ultrahigh-pressure eclogites from the ZK703 drillhole in the Donghai, eastern China. *Lithos* **52**, 35–50.

Zhang R. Y., Liou J. G., Zheng Y.-F. and Fu B. (2003) Transition of UHP eclogites to gneissic rocks of low-grade amphibolite facies during exhumation: evidence from the Dabie terrane, central China. *Lithos* **70**, 269–291.

Zhang Z. M., Xiao Y. L., Xu Z. Q., Hoefs J., Yang J. S., Liu F. L., Liou J. G. and Simon K. (2006a) UHP metamorphic rocks from the Chinese continental scientific drilling project: I. Petrology and geochemistry of the main hole (0–2,050 m). *Contrib. Mineral. Petrol.* **152**, 421–441.

Zhang Z. M., Liou J. G., Zhao X. D. and Shi C. (2006b) Petrogenesis of Maobei rutile eclogites from the southern Sulu ultrahigh-pressure metamorphic belt, eastern China. *J. Metamorph. Geol.* **24**, 727–741.

Zhao Z.-F., Zheng Y.-F., Gao T.-S., Wu Y.-B., Chen B., Chen F. K. and Wu F.-Y. (2006) Isotopic constraints on age and duration of fluid-assisted high-pressure eclogite-facies recrystallization during exhumation of deeply subducted continental crust in the Sulu orogen. *J. Metamorph. Geol.* **24**, 687–702.

Zhao Z.-F., Chen B., Zheng Y.-F., Chen R.-X. and Wu Y.-B. (2007) Mineral oxygen isotope and hydroxyl content changes in ultrahigh-pressure eclogite-gneiss contacts from Chinese Continental Scientific Drilling Project cores. *J. Metamorph. Geol.* **25**, 165–186.

Zheng Y.-F. (1989) Influence of the nature of the initial Rb–Sr system on isochron validity. *Chem. Geol.* **80**, 1–16.

Zheng Y.-F., Fu B., Xiao Y.-L., Li Y.-L. and Gong B. (1999) Hydrogen and oxygen isotope evidence for fluid–rock interactions in the stages of pre- and post-UHP metamorphism in the Dabie Mountains. *Lithos* **46**, 677–693.

Zheng Y.-F., Fu B., Gong B. and Li L. (2003) Stable isotope geochemistry of ultrahigh pressure metamorphic rocks from the Dabie–Sulu orogen in China: implications for geodynamics and fluid regime. *Earth Sci. Rev.* **62**, 105–161.

Zheng Y.-F., Wu Y.-B., Chen F. K., Gong B., Li L. and Zhao Z.-F. (2004) Zircon U–Pb and oxygen isotope evidence for a large-scale ^{18}O depletion event in igneous rocks during the Neoproterozoic. *Geochim. Cosmochim. Acta* **68**, 4145–4165.

Zheng Y.-F., Zhou J.-B., Wu Y.-B. and Xie Z. (2005a) Low-grade metamorphic rocks in the Dabie–Sulu orogenic belt: a passive-margin accretionary wedge deformed during continent subduction. *Int. Geol. Rev.* **47**, 851–871.

Zheng Y.-F., Wu Y.-B., Zhao Z.-F., Zhang S.-B., Xu P. and Wu F.-Y. (2005b) Metamorphic effect on zircon Lu-Hf and U–Pb isotope systems in ultrahigh-pressure eclogite-facies metagranite and metabasite. *Earth Planet. Sci. Lett.* **240**, 378–400.

Zheng Y.-F., Zhao Z.-F., Wu Y.-B., Zhang S.-B., Liu X. M. and Wu F.-Y. (2006) Zircon U–Pb age, Hf and O isotope constraints on protolith origin of ultrahigh-pressure eclogite and gneiss in the Dabie orogen. *Chem. Geol.* **231**, 135–158.

Zheng Y.-F., Zhang S.-B., Zhao Z.-F., Wu Y.-B., Li X. H., Li Z. X. and Wu F.-Y. (2007) Contrasting zircon Hf and O isotopes in the two episodes of Neoproterozoic granitoids in South China: implications for growth and reworking of continental crust. *Lithos* **96**, 127–150.

Zong K. Q., Liu Y. S., Liu X. M. and Zhang B. H. (2007) Trace elemental records of short-lived heating during exhumation of the CCSD eclogites. *Chin. Sci. Bull.* **52**, 813–824.

Associate editor: Alan D. Brandon